



Novel thienocycloalkylpyridazinones as useful scaffolds for acetylcholinesterase inhibition and serotonin 5-HT₆ receptor interaction

Battistina Asproni^{a,*}, Marco Catto^b, Giovanni Loriga^c, Gabriele Murineddu^a, Paola Corona^a, Rosa Purgatorio^b, Elena Cichero^d, Paola Fossa^d, Naomi Scarano^d, Antón L. Martínez^e, José Brea^e, Gérard A. Pinna^a

^a Department of Medicine, Surgery and Pharmacy, University of Sassari, Via Muroni 23/a, 07100 Sassari, Italy

^b Department of Pharmacy-Pharmaceutical Sciences, University of Bari Aldo Moro, Via E. Orabona 4, 70125 Bari, Italy

^c Institute of Biomolecular Chemistry, National Research Council, Traversa La Crucca 3, 07100 Sassari, Italy

^d Department of Pharmacy, Section of Medicinal Chemistry, School of Medical and Pharmaceutical Sciences, University of Genoa, Viale Benedetto XV, 3, 16132 Genoa, Italy

^e BioFarma Research Group, Centro Singular de Investigación en Medicina Molecular y Enfermedades Crónicas (CIMUS), Universidade de Santiago de Compostela, 15782 Santiago de Compostela, Spain

ARTICLE INFO

Keywords:

Acetylcholinesterase inhibitors
5-HT₆ receptor ligands
Multitarget-directed ligands
Alzheimer's disease
Thienocycloalkylpyridazinone derivatives

ABSTRACT

A library of eighteen thienocycloalkylpyridazinones was synthesized for human acetylcholinesterase (*hAChE*) and butyrylcholinesterase (*hBChE*) inhibition and serotonin 5-HT₆ receptor subtype interaction by following a multitarget-directed ligand approach (MTDL), as a suitable strategy for treatment of Alzheimer's disease (AD). The novel compounds featured a tricyclic scaffold, namely thieno[3,2-*h*]cinnolinone, thienocyclopentapyridazinone and thienocycloheptapyridazinone, connected through alkyl chains of variable length to proper amine moieties, most often represented by *N*-benzylpiperazine or 1-(phenylsulfonyl)-4-(piperazin-1-ylmethyl)-1*H*-indole as structural elements addressing AChE and 5-HT₆ interaction, respectively. Our study highlighted the versatility of thienocycloalkylpyridazinones as useful architectures for AChE interaction, with several *N*-benzylpiperazine-based analogues emerging as potent and selective *hAChE* inhibitors with IC₅₀ in the 0.17–1.23 μM range, exhibiting low to poor activity for *hBChE* (IC₅₀ = 4.13–9.70 μM). The introduction of 5-HT₆ structural moiety phenylsulfonylindole in place of *N*-benzylpiperazine, in tandem with a pentamethylene linker, gave potent 5-HT₆ thieno[3,2-*h*]cinnolinone and thienocyclopentapyridazinone-based ligands both displaying *hAChE* inhibition in the low micromolar range and unappreciable activity towards *hBChE*. While docking studies provided a rational structural explanation for AChE/BChE enzyme and 5-HT₆ receptor interaction, *in silico* prediction of ADME properties of tested compounds suggested further optimization for development of such compounds in the field of MTDL for AD.

1. Introduction

Acetylcholinesterase (AChE) belongs to the α/β hydrolase fold protein superfamily¹ whose principal physiological function is the rapid hydrolysis of acetylcholine (ACh) in the synapse and neuromuscular junction, resulting in the termination of nerve impulse. Low levels of ACh in the cerebral cortex and other brain areas appear to have a critical role in the development of cognitive and neurodegenerative disorders in Alzheimer's disease (AD, cholinergic hypothesis).² Butyrylcholinesterase (BChE), another cholinesterase present in the brain, has similar

biological function as AChE for hydrolysis of ACh in a healthy human brain, even if playing a minor role in regulating ACh levels. Indeed, the AChE activity is dominant in the healthy brain (80%), while the BChE activity becomes dominant in brain during the development of AD.^{3,4} Furthermore, it is noteworthy that AChE facilitates amyloid beta (Aβ) protein aggregation by the peripheral anionic binding site (PAS) of the enzyme⁵ and participates in the abnormal phosphorylation of the τ protein,⁶ thus playing a crucial role in the development and progression of AD. To date, current treatments of AD make use of drugs that can increase cholinergic neurotransmission by inhibiting AChE or/and

* Corresponding author.

E-mail address: asproni@uniss.it (B. Asproni).

<https://doi.org/10.1016/j.bmc.2023.117256>

Received 18 January 2023; Received in revised form 10 March 2023; Accepted 17 March 2023

Available online 21 March 2023

0968-0896/© 2023 The Authors. Published by Elsevier Ltd. This is an open access article under the CC BY license (<http://creativecommons.org/licenses/by/4.0/>).

BChE,⁷ which include donepezil,⁸ rivastigmine,⁹ and the alkaloid galantamine¹⁰ (Fig. 1). Unfortunately, although these drugs offer some cognitive improvements in AD, they can only slow down the progression of the disease and are effective only for a limited time. Furthermore, several adverse drug reactions associated with cholinesterase inhibition, such as nausea, diarrhea and vomiting may occur.¹¹ These findings, together with the increasing incidence of AD as the main cause of dementia, prompted intensive and dedicated search aiming at identifying novel safer cholinesterase inhibitors^{12,13} endowed of minimal adverse effects or new biological targets for the treatment of AD.¹⁴

Within this frame, the serotonergic system and several of its receptors (especially 5-HT_{1A}, 5-HT₄, 5-HT₆ and 5-HT₇) raised a great interest as important players influencing different aspect of cognitive dysfunction as cognitive deficits, learning and memory decline in neurodegenerative diseases.^{15–19} In particular, the localization of 5-HT₆ receptors mainly within the CNS in brain areas involved in learning and memory processes as striatum, hippocampus and cerebral cortex, contributed to the identification of such serotonin receptor subtype as a putative target for AD.^{17,20} Microdialysis studies have shown that blockade of 5-HT₆ receptors induced an increase of ACh levels, as well as reversed cognition deficits induced after the administration of anticholinergic agents.^{17,21} A plethora of studies evidenced that these effects are mediated by the involvement of multiple neurotransmitter systems as cholinergic, glutamatergic and GABAergic.^{22–25} Furthermore, blockade of 5-HT₆ receptors may result in other beneficial neuropharmacological effects for AD treatment as anxiolytic and antidepressant activity.^{26,27} The pharmacological relevance of 5-HT₆ receptor target for the treatment of AD emerged from Phase II clinical study highlighting the improved cognitive function elicited by the potent and selective 5-HT₆ antagonist idalopirdine in donepezil-treated patients with moderate AD.^{28,29} Fig. 2 depicts the structures of significant 5-HT₆ receptor antagonists belonging to different chemotypes.^{17,30}

Despite early positive findings, larger Phase III trials failed to demonstrate any significant impact on cognition for idalopirdine in combination to cholinesterase inhibitor donepezil.^{31,32} Beyond the inability of idalopirdine to provide satisfying effects in AD patients, several other issues, as a risk of elevated liver enzymes or vomiting may be attributed to its Phase III failure. However, the positive results observed in Phase II became the rationale for the design of multitarget-directed ligands (MTDL)³³ as cholinesterase inhibitors and 5-HT₆ receptor antagonists, potentially useful for treatment of AD. Accordingly, different classes of AChE/BChE inhibitor ligands with 5-HT₆ receptor antagonist properties have been synthesized, several of them endowed with anti-aggregation properties against amyloid-beta and tau or antioxidant/metal chelating activity.^{34–38} Such results may provide a promising starting point for further in-depth biological studies and for the development of an effective anti-AD therapy.

Several diverse molecular architectures suitable for cholinesterase interaction were reported in the literature.^{12,13} In particular, we focused our attention on a series of thienocycloalkylpyridazinones of general formula B (Fig. 3), sharing the tricyclic scaffold linked through linear polymethylene chains of variable length to an amine portion (Q), most

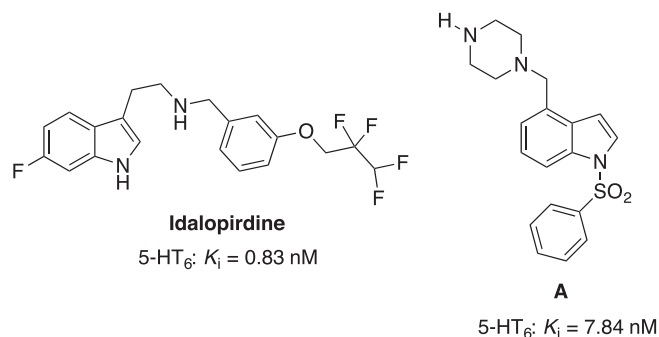


Fig. 2. Structure and K_i values of 5-HT₆ antagonists belonging to different chemotypes.

often represented by a substituted piperazine. Pharmacomodulation of thienocycloalkylpyridazinone nucleus in combination with a proper linker/amine moiety provided several compounds displaying high AChE inhibition in the low micromolar to sub-micromolar range and low selectivity over BChE that, in a few cases, was even inverted. Our structure–activity relationship (SAR) study evidenced the versatility of such tricyclic core as useful scaffold for interaction to target cholinesterases.³⁹ Compound 1, incorporating the thieno[2,3-*h*]cinnolinone core, emerged for its high affinity for AChE, accompanied by a low affinity for BChE.³⁹ Continuing with our interest in expanding structure–activity relationship (SAR) studies on AChE and/or BChE, we embarked on a study aimed to prepare new cholinesterase ligands related both to thienocycloalkylpyridazinones B and its representative derivative 1. Within this frame, taking into consideration the pharmacological relevance of serotonin receptors and particularly of 5-HT₆ for the treatment of neurodegenerative diseases as AD, the aim of this study was to combine AChE and/or BChE inhibition activity and 5-HT₆ receptor interaction. Thus, shift of the sulfur atom of the thieno[2,3-*h*]cinnolinone core in compound 1 from position 7 to 9 and homologation of the carbocyclic central ring of the tricyclic core, gave rise to novel thienocycloalkylpyridazinones, namely thieno[3,2-*h*]cinnolinone C, thienocyclopentapyridazinone D and thienocycloheptapyridazinone E. Looking at the reference compound 1, we planned the insertion of *N*-benzylpiperazine and simple alkyl/cycloalkyl amines, as well as the phenylsulfonyl-piperazin-indole derivative A (Fig. 2), endowed with high affinity for 5-HT₆ receptor.³⁰ Novel compounds that varied the tricyclic pyridazinone core, the amine moiety and the alkyl linker were designed (Tab. 1 and 2) for cholinesterases' inhibition and serotonergic interaction. In this paper, we report the synthesis of compounds 2a–l, 3a–e, 4a, together with preliminary aspects of their cholinesterase affinity, selectivity, serotonergic receptor affinity and biological activities and molecular modeling studies. In silico evaluation of the pharmacokinetic properties are reported, with the aim at gaining preliminary information concerning their potential drug-like profile.

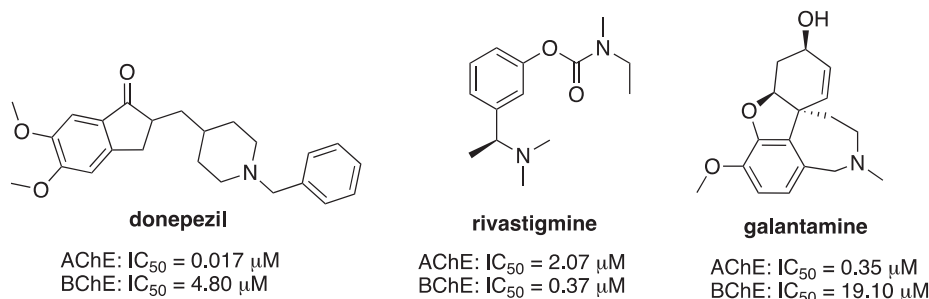


Fig. 1. Structures and IC₅₀ values of donepezil, rivastigmine and galantamine versus cholinesterases.

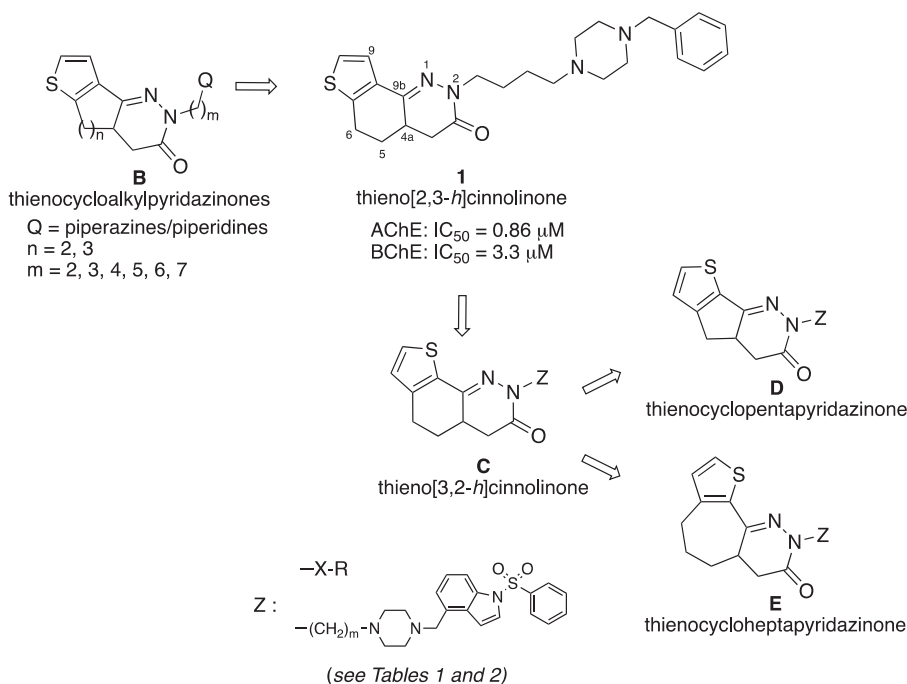


Fig. 3. Structure of thienocycloalkylpyridazinones.

2. Chemistry

The chemistry employed to prepare title compounds **2a-l**, **3a-e**, **4a** (Tab. 1 and 2) is outlined in Schemes 1-3, and profited from our consolidated experience in the synthesis of polycyclic pyridazinones.³⁹⁻⁴¹

Scheme 1 depicts the synthetic route to most of the title compounds presented in this paper, based on standard nucleophilic substitution reaction of bromine derivatives **5-15** and appropriate amines. Intermediates **5-15** were synthesized by alkylation of key tricyclic pyridazinones **2-4** with the appropriate alkyl dibromide, using, in most cases, phase-transfer conditions and were obtained in good yields. The new tricyclic pyridazinones **3** and **4** were synthesized following the procedure (Scheme 2) applied in our lab for the synthesis of thieno[3,2-*h*]cinnolinone **2**.⁴⁰ Accordingly, the starting ketones **16**^{42,43} and **17**⁴⁴ were submitted to Mannich reaction to furnish **18** and **19**, which were converted with NaCN in CH₃OH into the nitriles **20** and **21**. Hydrolysis of nitriles in refluxing HCl led to the γ -ketoacids **22** and **23** whose reaction with hydrazine hydrate afforded the desired pyridazinones **3** and

4. The synthesis of compound **2g** was accomplished by treatment of pyridazinone **2** with formaldehyde and *N*-benzylpiperazine (Scheme 3).

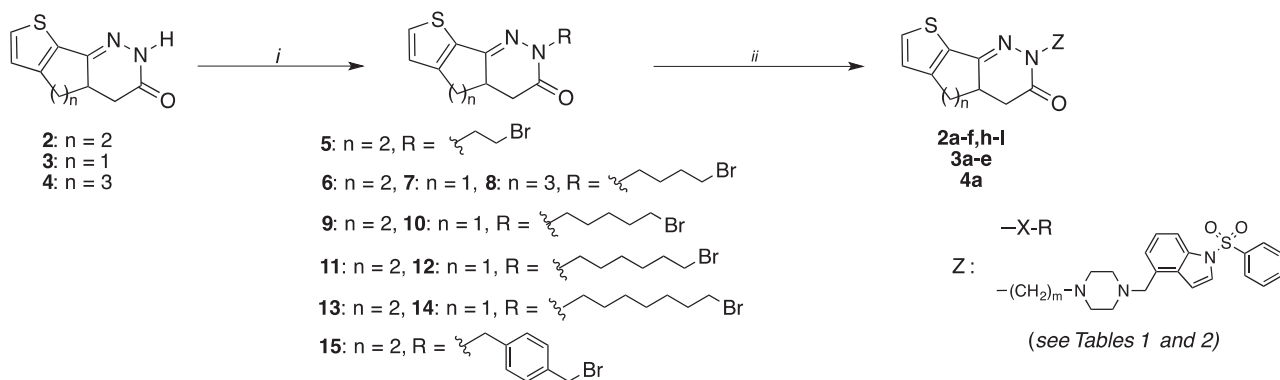
3. Biology

3.1. AChE and BChE inhibition assay.

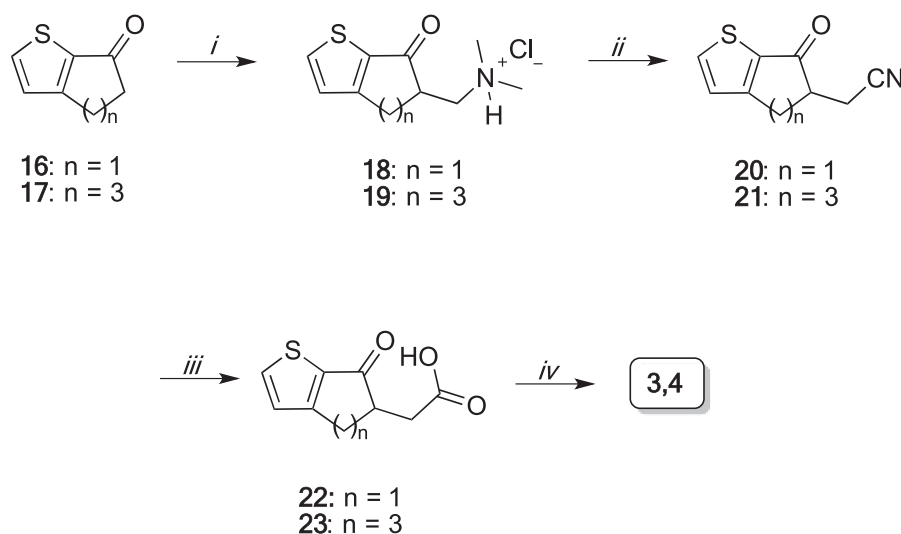
Compounds **2a-l**, **3a-e**, **4a** were tested for their inhibitory activity toward human isoforms of acetylcholinesterase (*hAChE*) and butyrylcholinesterase (*hBChE*) by the classical spectrophotometric Ellman's assay.⁴⁵ Inhibitory activities were determined as IC₅₀ values, except for less active compounds (% inhibition at 10 µM < 50%). Inhibition kinetics on *hAChE* of compound **2f** were determined at different concentrations of both inhibitor and acetylcholine substrate by using the Michaelis-Menten approach.

3.2. Serotonin receptor binding assays.

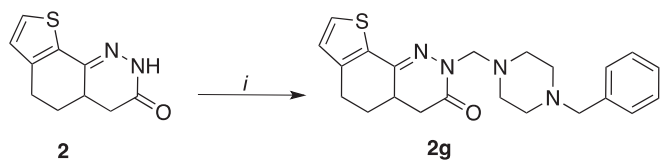
All title compounds were tested for their affinity in human HEK cell



Scheme 1. Reagents and conditions: *i*) method a: halogen derivative, NaH 60%, dry DMF, rt, 1 h (compound **5** and **8**); method b: halogen derivative, *n*-Bu₄NHSO₄, CH₂Cl₂, NaOH 28%, H₂O, 40 °C, 2.5 h (compounds **6**, **7**, **9-14**); method c: 1,4-bis(bromomethyl)benzene, K₂CO₃, CH₃CN, 80 °C, 30 h (compound **15**); *ii*) appropriate amine, K₂CO₃, KI, CH₃CN, 80 °C, 1 h.



Scheme 2. Reagents and conditions: *i*) CH_2O 37%, $(\text{CH}_3)_2\text{NH}\cdot\text{HCl}$, rt, Ac_2O , 75 °C, 4 h; *ii*) NaCN water solution, CH_3OH , 55 °C, 4 h; *iii*) HCl 6 M, 100 °C, 7 h; *iv*) $\text{NH}_2\text{-NH}_2\cdot\text{H}_2\text{O}$, EtOH, 80 °C, 3 h.



Scheme 3. Reagents and conditions: *i*) dry EtOH, CH_2O 37%, *N*-benzylpiperazine, N_2 , 80 °C, 3 h.

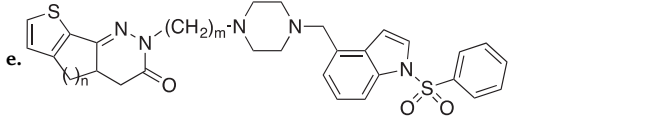
lines overexpressing 5-HT_{1A}, 5-HT₆ and 5-HT₇ receptors, by means of radioligand binding competition studies. [³H]-8-OH-DPAT, [³H]-LSD and [³H]-SB269970 were employed as radiolabeled ligands for 5-HT_{1A}, 5-HT₆ and 5-HT₇ receptors, respectively. Affinity data were expressed as the percentage of radioligand displacement at 10 μM. *K*_i values were calculated from concentration-response curves for those compounds showing a percentage of radioligand displacement higher than 43% at 10 μM. The affinity values for tested compounds are shown in Tables 1 and 2. Functional experiments on 5-HT₄ receptors were carried out in Hela-5-HT₄ cells, measuring the fluorescence change induced by calcium mobilization.

Table 1

Biological activity data of compounds **2a-h**, **3a**, **4a**.

Compd.	n	X	R	IC ₅₀ (μM) or (% inhibn. @ 10 μM)		K _i (nM) or (% inhibn. @ 10 μM)		
				<i>h</i> AChE	<i>h</i> BChE ^a	5-HT ₆	5-HT _{1A}	5-HT ₇
2a	2	(CH ₂) ₄		0.756 ± 0.010	(45 ± 3)	3298 ± 534	496 ± 117	995 ± 137
2b	2	(CH ₂) ₄	NMe ₂	6.36 ± 0.06	ni	(36 ± 4)	(37 ± 1)	(24 ± 4)
2c	2	(CH ₂) ₄	NEt ₂	2.93 ± 0.15	ni	(27 ± 2)	8631 ± 1696	(10 ± 1)
2d	2	(CH ₂) ₄		1.16 ± 0.04	(14 ± 1)	(33 ± 4)	3528 ± 508	(16 ± 1)
2e	2	(CH ₂) ₄		2.09 ± 0.08	(9 ± 2)	(30 ± 3)	4299 ± 1118	(18 ± 2)
2f	2	(CH ₂) ₂		0.170 ± 0.020	5.11 ± 0.08	1667 ± 639	1084 ± 164	(26 ± 6)
2g	2	CH ₂		13.6 ± 2.5	5.58 ± 0.43	(28 ± 2)	(24 ± 1)	(23 ± 2)
2h	2			3.65 ± 0.57	9.70 ± 1.70	1261 ± 240	786 ± 177	2108 ± 626
3a	1	(CH ₂) ₄		0.538 ± 0.052	(11 ± 1)	3969 ± 641	614 ± 85	1003 ± 199
4a	3	(CH ₂) ₄		1.23 ± 0.09	4.13 ± 0.43	1430 ± 183	414 ± 104	976 ± 137
Donepezil				0.016 ± 0.002	4.80 ± 1.00			

(^a), ni: no inhibition at 10 μM concentration.

Table 2
Biological activity data of compounds **2i-l**, **3b-e**


Comp.	m	n	IC_{50} (μ M)				
			<i>h</i> AChE	5-HT ₆	5-HT _{1A}	5-HT ₄	5-HT ₇
2i	4	2	7.61 ± 0.59	236 ± 83	2840 ± 773	ni	2009 ± 702
2j	5	2	4.44 ± 0.77	63 ± 13	(35 ± 1)	ni	1690 ± 628
2k	6	2	9.80 ± 1.21	102 ± 36	(23 ± 2)	(12 ± 2)	(33 ± 6)
2l	7	2	4.56 ± 0.42	87 ± 22	(33 ± 6)	(16 ± 4)	(43 ± 2)
3b	4	1	3.55 ± 0.87	193 ± 48	4610 ± 1525	(26 ± 4)	2018 ± 347
3c	5	1	6.89 ± 1.01	8.4 ± 2	3580 ± 1343	ni	1802 ± 305
3d	6	1	9.18 ± 0.49	68 ± 13	5160 ± 1405	ni	(39 ± 1)
3e	7	1	7.18 ± 1.49	80 ± 19	6620 ± 1604	ni	3759 ± 664
Methiothepin				1.3 ± 0.1			1.7 ± 0.3
GR113808						1.4 ± 0.2	
5-CT					0.2 ± 0.1		

(°), ni: no inhibition at 10 μ M concentration.

4. Results and discussion

4.1. AChE/BChE enzyme inhibition and serotonin receptor binding assay.

Compound **2a**, incorporating the thieno[3,2-*h*]cinnolinone core, exhibited high potency in inhibiting AChE activity, with an IC_{50} value ($IC_{50} = 0.76 \mu$ M) very similar to that of its positional isomer **1** ($IC_{50} = 0.86 \mu$ M), indicating that the shifting of sulfur atom from position 7 to 9 did not significantly influence the affinity for the enzyme. Notably, such modification induced loss of affinity for BChE (45% inhibition at 10 μ M, versus compound **1**, $IC_{50} = 3.3 \mu$ M).

Compared to **2a**, compounds **2b-e**, bearing smaller alkyl/cycloalkyl amines exhibited a slightly decreased affinity for AChE and an almost total loss of affinity for BChE, most likely due to the lack of benzyl portion responsible for a more efficient interaction at the enzyme binding site. Compounds **2f-h** were designed to investigate the effects on inhibition potency and selectivity at the target enzymes of the polymethylene linker joining the thieno[2,3-*h*]cinnolinone core with the

basic moiety. In particular, shortening of the polymethylene linker from 4 (compound **2a**) to 2 or 1 carbon units (compounds **2f**, **2g**) induced a significant impact on AChE/BChE affinity/selectivity. While **2f** exhibited the highest potency for AChE among all tested compounds ($IC_{50} = 0.17 \mu$ M), the homologue compound **2g** resulted 80-fold less potent than **2f** and, notably, endowed with the least AChE potency. Compound **2h**, sharing a *para*-xylyl linker with lower conformational flexibility if compared to **2a**, resulted in a 5-fold decreased affinity for AChE.

The inhibition mechanism of **2f** was assessed through an inhibition kinetics study by means of the Michaelis-Menten equation and the double reciprocal linearization according to Lineweaver-Burk (Fig. 4). From this study **2f** resulted in a competitive inhibitor with $K_i = 0.123 \pm 0.016 \mu$ M, thus evidencing a reversible interaction at the catalytic binding site of *h*AChE.

Homologation of thieno[2,3-*h*]cinnolinone core of **2a**, to give thienocyclopentapyridazinone **3a** and thienocycloheptapyridazinone **4a** induced a slight impact on AChE affinity. Looking at the BChE inhibition values, almost all compounds exhibited poor to low activity with a high degree of selectivity versus AChE, with the only exception of compound **2g**.

By pursuing our interest in expanding the biological activity of thienocycloalkylpyridazinones to 5-HT₆ receptors, novel derivatives were designed through molecular hybridization. In particular, based upon the high 5-HT₆ receptor affinity of 1-(phenylsulfonyl)-4-(piperazin-1-ylmethyl)-1*H*-indole compound A (5-HT₆ $K_i = 7.84$ nM, Fig. 2)³⁰ it was postulated that the introduction of phenylsulfonyl indole in place of benzyl as the structural element addressing 5-HT₆ activity, might provide new AChE ligands with mixed affinity at 5-HT₆ receptors. Thus, two series of compounds were prepared, namely the thieno[2,3-*h*]cinnolinones (**2i-l**) and the thienocyclopentapyridazinones (**3b-e**), Table 2.

The study at the target enzymes was extended at additional serotonergic receptors, namely 5-HT_{1A}, 5-HT₄ and 5-HT₇ receptors, in order to obtain a preliminary profile of selectivity within the wide 5-HT receptor (5-HTR) family. We decided to include in our assays these subtypes because of their recognized role in AD⁴⁶ and the presence in our molecules of main structural pharmacophoric elements for 5-HTR interaction, namely the indole moiety bound by a polymethylene bridge to a core tricyclic structure. 5-HT₄ subtype activates ACh release in the frontal cortex and hippocampus, with memory enhancing effects, and modulates GABA and dopamine homeostasis.⁴⁷ 5-HT₇ receptor has been recently described for its involvement in AD through enhancement of neuronal plasticity, neuroprotection from excitotoxicity, cognitive sustainment.⁴⁸ Concerning 5-HT_{1A} subtype, its modulation is by far recognized for the treatment of psychiatric disorders in AD;⁴⁹ nevertheless, its role in many neuronal networks⁵⁰ recommends to exclude, at a preliminary evaluation stage, possible undesired effects due to its inhibition.

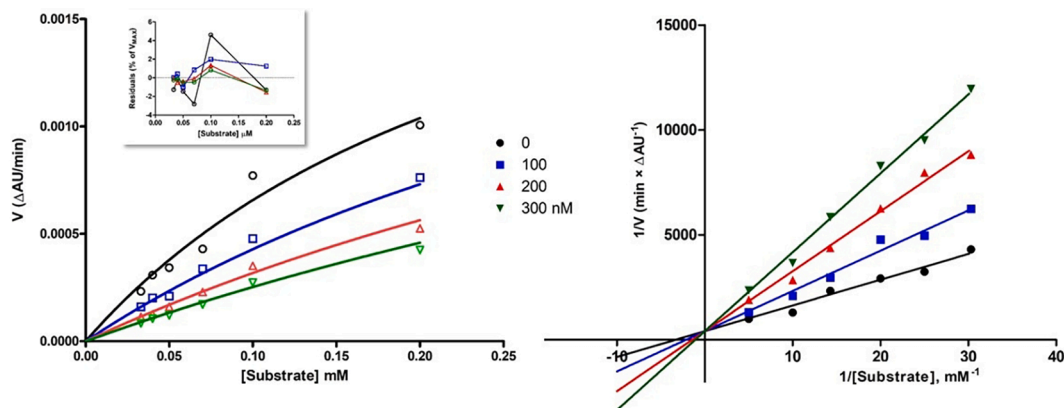


Fig. 4. Michaelis-Menten plot (left) and Lineweaver-Burk linearization (right) of AChE inhibition kinetics of **2f**. Inset: graph of residual % of V_{MAX} for competitive inhibition type.

Compounds **2i** and **3b**, featuring a linker of 4 carbon units as in **2a** and **3a**, exhibited interesting 5-HT₆ binding affinity reaching K_i values of 236 and 193 nM, respectively. Conversely, both exhibited decreased affinity for AChE, if compared to *N*-benzylpiperazine congeners **2a** and **3a**. Increasing the length of linker from 4 to 7 carbon units (compounds **2j-1** and **3c-e**) induced a significant impact on 5-HT₆ receptor interaction. In particular, looking at thienocyclopentapyridazinone-based derivatives **3c-e**, the pentamethylene chain appeared to be the most favorable spacer for 5-HT₆ receptor interaction, with the homologue **3c** reaching an outstanding K_i value of 8.4 nM, very close to that of 5-HT₆ ligand **A**. Even within the thieno[2,3-*h*]cinnolinone series **2j-1**, the pentamethylene-bearing derivative **2j** reached the lower K_i value of 63 nM, with an ameliorated AChE affinity if compared to **3c** (AChE **2j**: $IC_{50} = 4.44 \mu\text{M}$ versus **3c**: IC_{50} 6.89 μM). Concerning the other 5-HT subtypes, all phenylsulfonyl indole derivatives displayed high selectivity for target 5-HT₆, in some cases reaching up to three orders of magnitude. Notably, all of these indole-based derivatives retained fair AChE inhibition with IC_{50} s in the 3–10 μM range and showed unappreciable activity towards BChE (data not reported). Our SAR study highlighted that all the newly prepared compounds bearing the phenylsulfonyl indole motif behaved as potent and selective 5-HT₆ inhibitors with additional activity as AChE inhibitors.

For the sake of comparison, all the compounds from Table 1 were also tested on serotonin receptors, excluding 5-HT₄. Interestingly, reference compounds **2a**, **3a** and **4a** resulted in poorer 5-HT₆ but increased 5-HT_{1A} and 5-HT₇ potencies, thus displaying a slight selectivity for 5-HT_{1A}, although with submicromolar K_i values. Shortening the polymethylene bridge (**2f**, **2g**) had an overall detrimental effect on 5-HT receptors, while pruning the basic distal moiety (**2b-e**) resulted in an almost complete loss of activity.

Fig. 5 summarizes and highlights the general effects of structural changes on cholinesterases/serotonine subtype receptors activities, carried out on thienocycloalkylpyridazinones. The results of our SAR study, in terms of multitarget profile, led to the identification of compound **2j**, featuring the phenylsulfonyl-indol-piperazine motif in tandem with the thieno[3,2-*h*]cinnolinone core, connected with a pentamethylene linker, as the best compromise achieved in terms of multitarget affinity.

These features confirmed the role of phenylsulfonyl indole moiety as a key structural element for 5-HT₆ selectivity, and at the same time the potential of further development of this class of compounds as multitarget agents for AD-related biological targets.

4.2. Molecular modeling studies

In order to elucidate the main modes of interaction of all synthesized ligands with the targets under investigation, we proceeded with molecular docking calculations, starting from the X-ray crystallographic structures of *h*AChE (PDB code = 7E3H)⁵¹ and *h*BChE enzymes (PDB code = 4BDS).⁵² In particular, the three-dimensional structures of the two proteins were detailed in presence of the ligands donepezil (7E3H) and tacrine (4BDS), respectively. This piece of information allowed us to apply a re-cross docking procedure for the 7E3H and 4BDS co-crystallized inhibitors in order to evaluate the most adequate docking protocol to be exploited for simulating the experimental data, based on a procedure described in the literature.⁵³ Herein, the two series of re-cross docking calculations were managed thanks to MOE software Dock module (see the experimental section for details).⁵⁴

The top five best scored docking positioning obtained for donepezil and tacrine as *h*AChE and *h*BChE inhibitors, as docked within the aforementioned complexes are shown in Table S1. Among these, the best scored conformers turned to be fully comparable to the co-crystallized tacrine and donepezil conformers (see Fig. S1), giving a good validation of the applied docking protocol.

Thus, the following molecular docking studies involving the newly designed series of compounds, have been performed applying the same docking protocol based on the 7E3H and 4BDS PDB codes, by MOE Dock (the corresponding scoring functions related to these docked compounds are listed in Tables S2-S3).

As regards the *h*AChE inhibition, the reference compound donepezil was engaged in several hydrophobic and π - π stacking with the enzyme cavity involving: (i) the inhibitor benzyl group and Trp86, (ii) the terminal bicyclic core and Tyr72, Tyr124, Trp286, Tyr341, Leu289. In addition, the previously mentioned benzyl ring displayed also a further cation- π contact with the surrounding His447 while the central piperidine ring experienced cation- π stacking with Trp86 and Tyr337 and an ionic interaction with Asp74, thanks to the protonated nitrogen atom of the inhibitor (Fig. S2).

As a result, the choice of at least two terminal aromatic fragments properly tethered to a central protonatable group is thought to guarantee the design of promising AChE inhibitors, able to feature a number of molecular interactions with the described highly aromatic enzyme cavity. Accordingly, among the newly designed compounds, those bearing the benzyl-substituted piperazine group tethered by an aliphatic chain spacer (ideally from two to four carbon atoms) to the terminal tricyclic aromatic ring proved to be the most promising (see **2a**, **2f**, **3a**

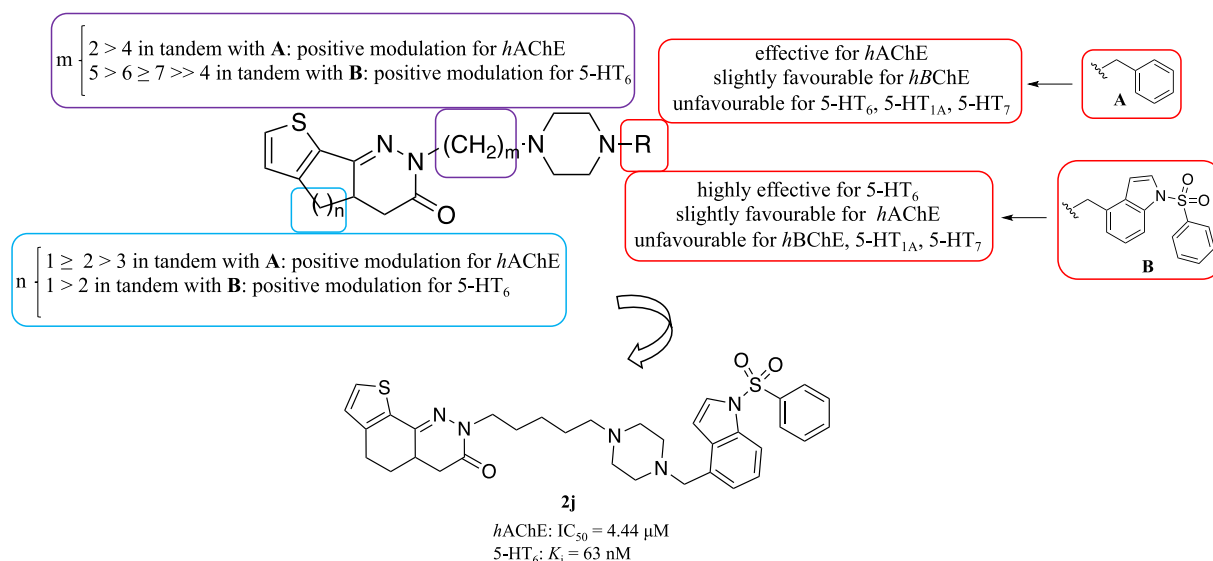


Fig. 5. SAR of thienocycloalkylpyridazinones on cholinesterases/serotonine subtype receptors.

and **4a**; $hAChE$ IC_{50} = 0.17–1.23 μ M). The following structure–activity relationship (SAR) discussion in terms of molecular modeling data has been developed based on compound **2a**, taken as representative of the most developed chemical series of analogues herein proposed. As shown in Fig. 6, compound **2a** ($hAChE$ IC_{50} = 0.756 μ M), featuring a four carbon atom aliphatic chain as spacer between the terminal six-membered carbocyclic-based core and the terminal benzyl-substituted piperazine group, showed a quite comparable docking mode with respect to the donepezil bioactive conformer.

While the terminal benzyl group of **2a** was engaged in π - π stacking with Trp86 and Tyr133, the aliphatic chain and the main tricyclic core were properly folded surrounding and simulating the positioning featured by the reference donepezil. In this way the compound was allowed to display a number of hydrophobic contacts with Phe297 and Tyr341, thanks to the aliphatic chain, and π - π stacking between the thieno-containing tricyclic ring and Tyr72, Trp286. The protonated nitrogen atom of the piperazine ring of **2a** was projected towards the oxygen atom of the Tyr337 backbone. On this basis, while the reported contacts proved to guarantee the $hAChE$ inhibition as exerted by compound **2a**, the lower potency value of this inhibitor (**2a**; $hAChE$ IC_{50} = 0.756 μ M), in comparison to that of donepezil ($hAChE$ IC_{50} = 0.017 μ M), might rely on a lower number of π - π stacking than the reference compound and on the absence of ionic interaction involving residue Asp74. Despite of this, the choice of a four-carbon atoms aliphatic spacer, led to most effective $hAChE$ inhibitor among the newly synthesized, thus supporting and experimentally validating the reported docking study. On the other hand, the introduction of a five-membered carbocyclic core in place of the previous and bulkier six-membered one featured by **2a**, led to the analogue **3a** ($hAChE$ IC_{50} = 0.538 μ M), endowed with a comparable potency as $hAChE$ inhibitor. Indeed, the related best scored **3a** docking pose was also efficiently overlapped onto the bioactive pose featured by donepezil (see Fig. 7).

Maintaining the six-membered carbocyclic central ring of the tricyclic main core and inserting a shorter aliphatic spacer between the tricyclic scaffold and the terminal benzyl group, led to the less and to the most potent analogues of the series, **2g** (one carbon atom-based spacer; $hAChE$ IC_{50} = 13.6 μ M) and **2f** (two carbon atom-based spacer; $hAChE$ IC_{50} = 0.17 μ M), respectively. Notably, the presence of only one carbon atom tethering the piperazine ring and the tricyclic core (compound **2g**) shifted the terminal tricyclic pendant with respect to the donepezil

bicyclic ring. This feature impaired the number of hydrophobic contacts with the surrounding residues, while the choice of a two carbon atom-based spacer, as featured by **2f**, was the most advantageous making the molecule able to fulfill perfectly the positioning of the benzyl portion as well as of the bicyclic core of the reference compound donepezil (see Fig. S3). This kind of positioning allowed the compound to achieve also a ionic interaction between the protonated nitrogen atom of the piperazine ring and Asp74 residue.

The search of putative $hBChE$ inhibitors led to the novel compound **4a** as the most interesting derivative among the newly developed compounds, even if endowed of low affinity for $hBChE$ with IC_{50} = 4.13 μ M, close to that of ligand **1** (IC_{50} = 3.3 μ M). Its calculated docking positioning (see Table S3) was analyzed and compared with the bioactive conformation featured by tacrine, as reference compound co-crystallized within the enzyme catalytic site (PDB code 4BDS).

According to our docking results, the $hBChE$ inhibitor tacrine was stabilized within the enzyme binding site by: (i) π - π stacking involving the compound aromatic portion and the surrounding residues Tyr332, Trp430 and Tyr440 and (ii) hydrophobic contacts between the tacrine carbocyclic group and Trp82, Thr120 and Tyr128 (see Fig. S4, left side).

In addition, the protonated nitrogen atom of the compound pyridine ring, was H-bonded to the oxygen atom of the His438 carbonyl group, thus properly arranging the compound at the enzyme crevice.

Further molecular docking calculations of the $hBChE$ inhibitor donepezil ($hBChE$ IC_{50} = 4.80 μ M) allowed to explore the putative docking mode of a more flexible chemotype with respect to the rigid scaffold experienced by tacrine. In addition, donepezil was also taken into account as reference compound for the biological assays and for the previous SAR discussion about the herein disclosed new anticholinesterase agents.

Based on our results, the benzyl substituent of donepezil was engaged in π - π stacking with Trp430 and Tyr440, while the bicyclic core of the compound was projected towards Gly117, Thr120, Ser198 and His438 detecting van der Waals contacts (see Fig. S4, right side). This kind of positioning was partially superposed with that of the co-crystallized ligand by means of the donepezil aromatic ring and was allowed by the presence of the protonated nitrogen atom on the piperidine ring of the inhibitor. Indeed, this turned in intra-molecular cation- π stacking with the inhibitor bicyclic ring, leading to the described folded positioning (U-shape) and contacts of the molecule.

As regards the novel derivatives herein described, compound **4a**, bearing a seven-membered carbocyclic central ring and a four-carbon atom-containing spacer, also showed a similar positioning (see Fig. 8, left side). Indeed, the benzyl-piperazine group of **4a** highly mimicked the positioning featured by the benzyl piperidine moiety of donepezil, displaying the same π - π stacking with Tyr332, Trp430 and Tyr440. Moreover, the folded terminal tricyclic ring overlapped the bicyclic one of donepezil, thus occupying the enzyme pocket delimited by Gly117, Thr120, Ser198 and His438.

Accordingly, in the experimental tests, **4a** resulted the most interesting $hBChE$ inhibitor among the newly developed compounds, featuring a comparable potency value with respect to donepezil.

The key role played by the introduction of (i) proper extended aliphatic chains and (ii) the dimension of the tricyclic ring, was confirmed by the lower potency trend as $hBChE$ inhibitors experienced by the analogue **3a** ($hBChE$ = 11% inhibition, @ 10 μ M) featuring a five-membered carbocyclic ring, and **2f** ($hBChE$ IC_{50} = 5.11 μ M), bearing a six-membered carbocyclic central ring in tandem with a two-carbon atom spacer. As shown in Fig. 8 (right side), compound **2f** maintained the previously cited U-shape thanks to the intra-molecular cation- π contact involving the piperazine protonated nitrogen and the terminal tricyclic ring. The compound displayed an adequate positioning within the enzyme pocket if compared with that of donepezil and of the most potent analogue **4a**.

These results highlight once again the aforementioned structural requirements of the inhibitor: the ligand should be folded and should

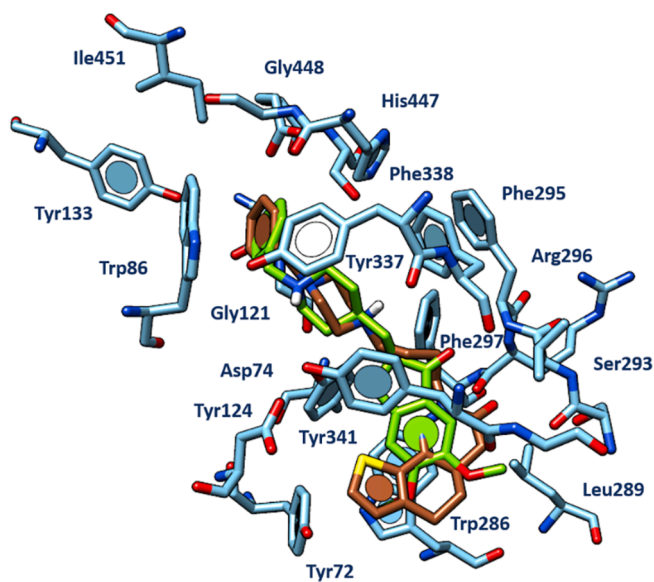


Fig. 6. Docking mode of the newly designed **2a** within the 7E3H PDB code. The $hAChE$ inhibitor has been reported in brown, in presence of the co-crystallized donepezil (C atom; green).

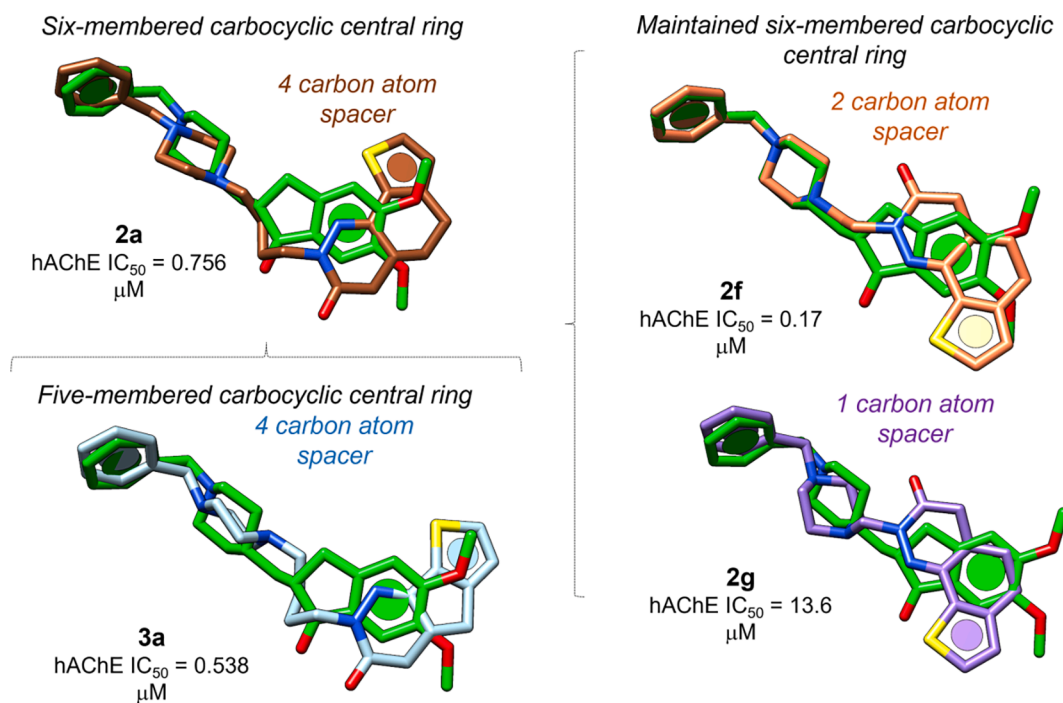


Fig. 7. Scheme of the applied structural variation at the prototype 2a (C atom; brown) leading to the highly related analogues 3a (C atom; cyan), 2f (C atom; orange) and 2g (C atom; purple) in tandem with the related hAChE inhibitory potency values. The figure reports the best pose of each ligand as derived from docking calculations. The X-ray crystallographic pose of donepezil in hAChE is depicted in green (PDB code = 7E3H).

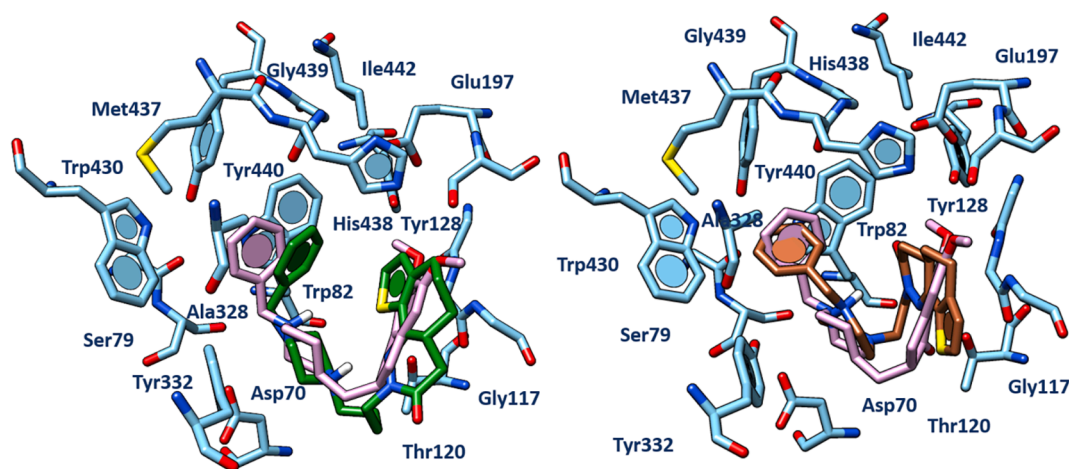


Fig. 8. Docking mode of the best scored donepezil conformer (C atom; light pink) within the 4BDS PDB code superimposed with inhibitors 4a (C atom; deep green) (left) and 2f (C atom; brown) (right). The most relevant amino acids involved in the hAChE-inhibitor molecular interactions are reported and labelled (4.5 Å far from the ligand).

show adequate occupancy of the enzyme cavity, so as to achieve van der Waals contacts with Gly117, Thr120, Ser198 and His438.

To pursue new hints for the design of further compounds conceivably endowed with 5-HT₆ targeting ability, we deemed interesting also exploring the docking mode of most potent inhibitors 3c and 2j. In order to achieve more comprehensive information, docking studies of the serotonergic antagonist methiothepin (5-HT₆ K_i = 1.3 nM), taken as reference compound, were also performed. The corresponding scoring function values obtained for the best ranked poses are shown in Table S4.

In absence of X-ray crystallographic data of the serotonergic 5-HT₆ receptor, we relied on the protein model as generated by AlphaFold protein structure database.^{55,56} This resource has been reported in literature as a very recent and useful tool for the accurate prediction of

tridimensional protein structures, based on deep learning methods.^{57,58} Then, in order to identify the putative 5-HT₆ binding site, structural similarity with the homologous protein 5-HT_{1A} was evaluated. In this way we could rely on our previous knowledge about the 5-HT_{1A} binding sites.

Briefly, in previous papers some of us reported deep molecular docking studies on several chemotypes endowed with 5-HT_{1A} targeting ability⁵⁹ such as dioxolane-based compounds and spiroderivatives, whose affinity trend towards the mentioned biological target was supported by a proper basic feature of the ligand, as interacting with a conserved aspartic acid (Asp116).^{60,61} Accordingly, a number of studies from literature reported a unique receptor site involved in the 5-HT_{1A} full agonists, partial agonists and antagonists binding involving Asp116,^{62,63} in accordance with our previous computational results.

Herein, based on the structural similarity between 5-HT_{1A} and 5-HT₆ receptors (pairwise percentage residue identity PPRI = 25% calculated by MOE software), we planned to identify the putative 5-HT₆ binding site by means of a consensus approach, initially involving the search of the putative druggable cavities calculated by the MOE Site Finder tool.⁵⁴ Then, the resulting information was compared with that obtained on the basis of the two proteins conserved residues analysis. Indeed, the putative 5-HT₆ binding site was identified by a comparison of the previously described 5-HT_{1A} binding site with the corresponding 5-HT₆ cavity. As a consequence, at the putative receptor binding cavity, the previously mentioned 5-HT_{1A} key residue Asp116 corresponded to the residue Asp106 in the 5-HT₆ 3D-model.

According to our calculations, the 5-HT₆ antagonist methiothepin (chosen as template) was engaged in a salt bridge between the protonated nitrogen atom of the piperazine group and the carboxylic function of Asp106, while the bulky tricyclic ring featured π - π stacking and van der Waals contacts with Phe284, Phe285 and Val107, Cys110, Val189, Ala192, respectively (see Fig. 9, left side).

Among the newly developed derivatives, compound 3c (5-HT₆ K_i = 8.4 nM) emerged as the most potent 5-HT₆ ligand, if compared to the other analogues, maintaining the required key contact with Asp106 (see Fig. 9, right side). Indeed, the protonated nitrogen atom of the piperazine guaranteed the required salt bridge with the conserved Asp106, while the arylsulfonamide portion was projected towards the hydrophobic residues, Cys110, Leu182 and Phe285. The presence of the five-carbon atom spacer tethered to the piperazine ring allowed to arrange the terminal tricyclic core in a deep pocket delimited by Asn86, Trp102 and Gln179. In this way, the same tricyclic ring was able to perform efficient interactions within the receptor binding relying on hydrophobic contacts.

The analogue 2j (5-HT₆ K_i = 63 nM), exhibiting the six-membered ring-based tricyclic core instead of the five-membered ring of 3c, maintained a lower 5-HT₆ targeting ability, due to weak ionic interactions involving the protonated piperazine nitrogen atom of the ligand and the key residue Asp106 (see Fig. 10, left side).

The bulkier 2j terminal tricyclic ring reversed the ligand docking positioning, with respect to 3c, moving the six-membered ring and the aryl sulfonyl group towards Val107, Val189, Phe284, Phe285 and Val29, Arg181, Trp307, respectively. This allowed the compound to detect van der Waals contacts with the biological target, even if with expense of π - π stacking.

Interestingly, 2j (hAChE IC₅₀ = 4.44 μ M) experienced slightly

ameliorated AChE inhibitory ability if compared to 3c (hAChE IC₅₀ = 6.89 μ M), opening the possibility for the design of further new analogues as dual acting compounds. Indeed, the choice of the six-membered ring in presence of the five carbon atom-based spacer, as shown by 2j, properly fulfilled the steric requirements of the enzyme crevice (see Fig. 10, right side). According to our calculations, the folded positioning featured by 2j guarantees the proper occupancy of the enzyme cavity, moving the tricyclic ring and the sulfonyl aryl-based group in proximity of Tyr337, Phe338 and Leu76, Trp286, Tyr341, respectively. This turns in a number of van der Waals and π - π stacking with the enzyme, in tandem with the salt-bridge involving the protonated piperazine nitrogen and the Asp74 side chain.

4.3. In silico prediction of ADME properties

As deeply described in the literature,^{64–66} the process of drug discovery takes advantage of the absorption, distribution, metabolism, excretion properties (ADME) in silico prediction. In the search of novel promising hit compounds to be further developed as anti-AD agents, herein we evaluated in silico pharmacokinetic properties (ADME parameters) of the new 2–4 series. The results are shown also for the drugs donepezil and methiothepin.

Thus, we considered putative violation of the well-known Veber' rule⁶⁷ and Lipinski' rule,⁶⁸ as prediction for logarithmic ratio of the octanol–water partitioning coefficient (cLogP), the molecular weight (MW) of derivatives, for the H-bonding acceptor number (N_{accH}), or donor groups (N_{donH}), and for the number of rotatable bonds (nRot_{bond}). The topological polar surface area (TPSA) and putative oral bioavailability as a percentage (F%) have been also estimated (see Table S5). Based on the Lipinski's rule, drug-like compounds feature MW < 500, cLogP < 5, HBA < 10 and HBD < 5, while the rule proposed by Veber represents drug bioavailability as nRot_{bonds} \leq 10, sum of HBA and HBD < 12 and for TPSA values \leq 140 \AA^2 .

According to our pharmacokinetic (PK) parameters prediction, all the derivatives fulfil both the Lipinski's rule and the Veber's rule, with the exception of the 2i, 2j, 2k, 2l and 3b-e series of compounds (see the nRot_{bond} and/or MW descriptor(s) in Table S5).

Then, in silico prediction of ADME parameters was also performed taking into account human intestinal absorption (HIA), estimation of the plasmatic protein binding event (%PPB), volume of distribution (Vd), ligand affinity toward human serum albumin (LogK_a HSA), prediction of the ability to pass the blood brain barrier (BBB) (see Table S6).

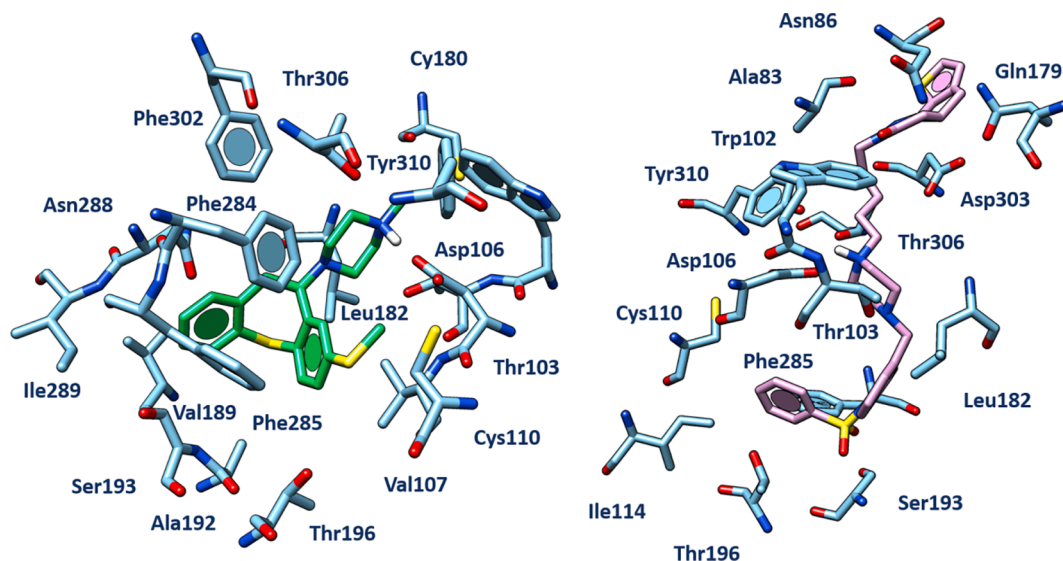


Fig. 9. Docking mode of the best scored methiothepin conformer (C atom; light green) within the human 5-HT₆ model (left) and of 3c (C atom; light pink) (right). The most relevant amino acids involved in the ligand-receptor interactions are reported and labelled (4.0 \AA far from the ligand).

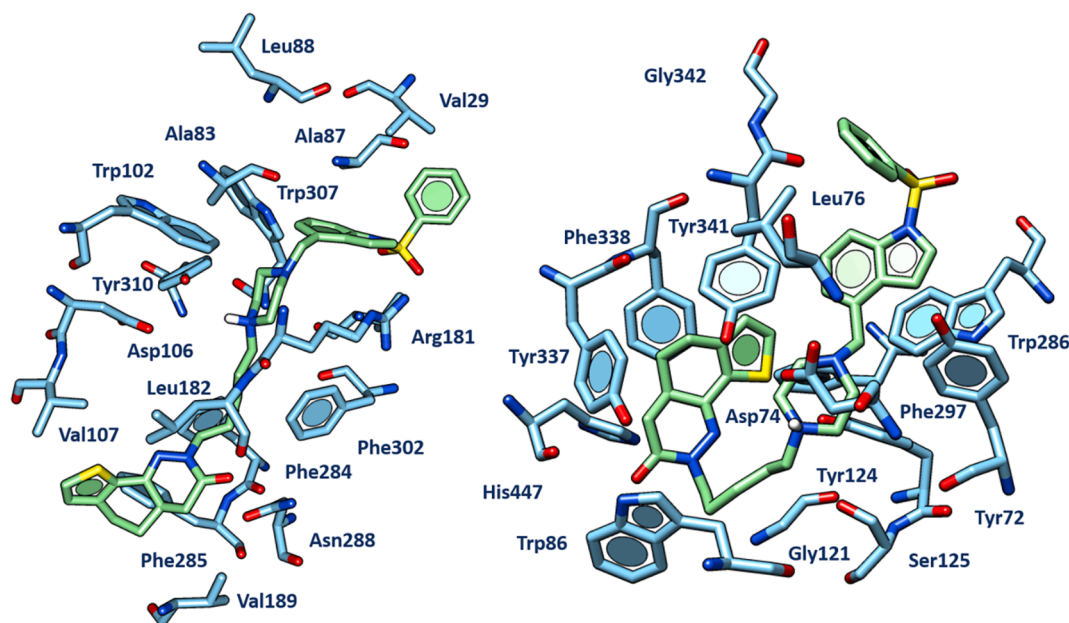


Fig. 10. Docking mode of the best scored **2j** conformer (C atom; light green) within the human 5-HT₆ model (left) and the hAChE as 7E3H PDB code (right). The most relevant amino acids involved in the ligand-protein interactions are reported and labelled (4.0 Å far from the ligand).

As shown in Table S6, all the newly developed compounds are highly absorbed (HIA% = 100%), being the most effective as hAChE/BChE inhibitors (**2a-h**, **3a**, **4a**) also able to pass the blood brain barrier (BBB). Conversely, the novel 5-HT₆ antagonists are predicted as inactive at the CNS, suggesting for further PK optimization as prosecution of this work.

5. Conclusions

The design of MTDL for the development of an effective anti-AD therapy, currently is highly pursued by the scientific community, due to several limitations of standard therapy which is based on the use of AChE inhibitors. Within this frame, using a consolidated experience in the synthesis of thienocycloalkylpyridazinones, we designed and synthesized novel MTDL acting as AChE or/and BChE inhibitors endowed of 5HT₆ receptor antagonist properties. The results presented herein highlight the suitability of thieno[3,2-*h*]cinnolinone, thienocyclopentapyridazinone and thienocycloheptapyridazinone as useful architectures for interaction with target cholinesterase enzymes/5-HT₆ serotonin receptor subtype, through the modulation of the amine moiety and the alkyl spacer. In particular, the *N*-benzylpiperazine in tandem with a four or two-carbon atom spacer was the preferred modification giving potent hAChE inhibitors **2a**, **2f**, **3a**, **4a** with IC₅₀ in the 0.17–1.23 μM range and low to poor activity versus hBChE (IC₅₀ = 4.13–9.70 μM). Docking studies provided a rational structural explanation for the ability of these novel derivatives to act preferentially as AChE inhibitors.

The introduction of phenylsulfonyl indole as favorable element for 5-HT₆ activity, in place of benzyl- on thieno[3,2-*h*]cinnolinone and thienocyclopentapyridazinone scaffolds evidenced an objective difficulty in obtaining multitarget ligands with potent AChE or/and BChE efficacy. SAR and docking studies conducted on both tricyclic-based derivatives allowed us to identify the phenylsulfonyl indole-based derivative **3c**, featuring the thienocyclopentapyridazinone scaffold in tandem with five carbon atom spacer, as the most potent and selective 5-HT₆ receptor ligand (5-HT₆ K_i = 8.4 nM; hAChE IC₅₀ = 6.89 μM; unappreciable activity versus hBChE). While our results confirmed the role of phenylsulfonyl indole moiety as a key structural element for 5-HT₆ selectivity, it will be necessary to investigate the mode of action of most potent derivatives by means of functional assays and animal models of scopolamine-induced memory impairment. The modulation of the size of the tricyclic core appeared to have some impact on AChE with

compound **2j** (5-HT₆ K_i = 63 nM; hAChE IC₅₀ = 4.44 μM) endowed with slightly ameliorated AChE inhibitory ability compared to the homologue **3c**. Such compound represents the best compromise achieved in terms of affinity for AChE enzyme and 5-HT₆ receptor subtype. This affinity trend may suggest there is room for possible further development of such compounds as MTDL for the treatment of AD.

In silico prediction of ADME properties conducted on **2a-l**, **3a-e**, **4a**, suggested further structural refinement for pharmacokinetic optimization, along with further in-depth pharmacological studies, determination of intrinsic toxicity, as an ideal prosecution of this work in the field of MTDL.

6. Experimental section

6.1. Chemistry

6.1.1. General methods

All moisture-sensitive reactions were conducted in anhydrous solvents (Sigma-Aldrich) under dry nitrogen atmosphere. All solvents and reagents were obtained from Sigma-Aldrich, Lancaster, or Merck and used without further purification. Reactions were monitored by analytical thin-layer chromatography (TLC) using Merck silica gel 60 TLC plates F254 and were visualized by UV light. Flash chromatography (FC) was performed using Merck silica gel 60 (230–400 mesh ASTM). Melting points were obtained on a Koffler melting point apparatus and are uncorrected. IR spectra were recorded as thin films on NaCl plates or as KBr pellets with a Jasco FT/IR 460 plus spectrophotometer and are expressed ν (cm⁻¹). NMR spectra were taken on a Bruker AVANCE III Nanobody 400 MHz spectrometer with ¹H and ¹³C being observed at 400 and 100.6 MHz, respectively. Chemical shifts for ¹H and ¹³C spectra are reported in δ (ppm) downfield from tetramethylsilane, and coupling constants (J) are expressed in Hertz. Multiplicities are recorded as s (singlet), br s (broad singlet), d (doublet), t (triplet), dd (doublet of doublets), m (multiplet). Electron ionization mass spectra (70 eV) were recorded with an Agilent 6850–5973 MSD gas chromatograph-mass spectrometer. High-resolution mass spectra (HRMS) were acquired on a Thermo Finnigan Q Exactive instrument with API-HESI source. Elemental analyses were performed with a PerkinElmer 2400 analyzer, and results were within \pm 0.3% of the calculated values. Compounds **A**,³⁰ **2**,⁴⁰ **16**^{42,43} and **17**⁴⁴ were synthesized as reported in the literature.

6.1.2. General procedure I. Synthesis of Mannich bases **18,19**

A mixture of dimethylamine hydrochloride (1.3 equiv.) in 37% formaldehyde (1.3 equiv.) was stirred at room temperature for 0.5 h. Acetic anhydride (4.9 equiv.) was dropwise added at 30–35 °C and the mixture was kept at 70–75 °C for 1 h. The appropriate ketone (**16** or **17**, 1 equiv.) was added and the whole stirred at 70–75 °C for 3 h. After cooling, the solution was evaporated under reduced pressure and the resulting crude residue was triturated with ether to afford the desired product, which was used in the next reaction with no further purification.

6.1.2.1. N,N-dimethyl-1-(6-oxo-5,6-dihydro-4H-cyclopenta[b]thiophen-5-yl)methanaminium Chloride (18). Compound **18** was synthesized by following general procedure I starting from 4,5-dihydro-6H-cyclopenta[b]thiophen-6-one **16** (1.30 g, 9.40 mmol) in 62% (1.35 g) yield; white powder; mp 170–171 °C. ¹H NMR (400 MHz, DMSO-*d*₆, δ/ppm): 2.81 (s, 6H); 3.13 (dd, 1H, *J* = 2.8 and 17.6 Hz); 3.35–3.40 (m, 2H); 3.47 (dd, 1H, *J* = 3.6 and 13.2 Hz); 3.62–3.66 (m, 1H); 7.30 (d, 1H, *J* = 4.8 Hz); 8.38 (d, 1H, *J* = 4.8 Hz); 10.92 (bs, 1H). ¹³C NMR (100 MHz, DMSO-*d*₆, δ/ppm): 29.7 (CH₂); 34.0 (CH); 48.2 (CH₃); 48.4 (CH₃); 57.5 (CH₂); 124.7 (CH); 138.4 (C); 147.2 (CH); 168.4 (C); 194.6 (CO).

6.1.2.2. N,N-dimethyl-1-(8-oxo-5,6,7,8-tetrahydro-4H-cyclohepta[b]thiophen-7-yl)methanaminium Chloride (19). Compound **19** was synthesized by following general procedure I starting from 4,5,6,7-tetrahydro-8H-cyclohepta[b]thiophen-8-one **17** (0.60 g, 3.61 mmol) in 87% (0.81 g) yield; white powder; mp 114–142 °C, dec. ¹H NMR (400 MHz, CDCl₃, δ/ppm): 1.56–1.75 (m, 2H); 2.23–2.45 (m, 2H); 2.74 (d, 3H, *J* = 4.8 Hz); 2.89 (d, 3H, *J* = 4.8 Hz); 2.95–3.15 (m, 3H); 3.56–3.65 (m, 1H); 3.85–3.96 (m, 1H); 6.97 (d, 1H, *J* = 4.8 Hz); 7.56 (d, 1H, *J* = 4.8 Hz); 11.09 (bs, 1H). ¹³C NMR (100 MHz, CDCl₃, δ/ppm): 25.0 (CH₂); 28.4 (CH₂); 28.6 (CH₂); 42.2 (CH); 45.2 (2 × CH₃); 57.9 (CH₂); 131.3 (CH); 133.2 (CH); 139.0 (C); 151.8 (C); 192.7 (CO).

6.1.3. General procedure II. Synthesis of nitriles **20, 21**

To a solution of appropriate Mannich base (**18** or **19**, 1 equiv.) in CH₃OH (5 mL per 2.59 mmol of Mannich base) an aqueous solution of NaCN (5.5 equiv.) was dropwise added at room temperature and the whole stirred at 55 °C for 4 h. The mixture was poured into ice water and extracted with CHCl₃. The organic phase was washed with H₂O, dried and evaporated to give the desired product, which was used in the next reaction with no further purification.

6.1.3.1. 2-(6-oxo-5,6-dihydro-4H-cyclopenta[b]thiophen-5-yl)acetonitrile (20). Compound **20** was synthesized by following general procedure II starting from **18** (4.40 g, 19.00 mmol) in 85% (2.86 g) yield; brown oil. IR (ν/cm⁻¹): 1701 (CO); 2249 (CN). ¹H NMR (400 MHz, CDCl₃, δ/ppm): 2.64 (dd, 1H, *J* = 8.0 and 16.8 Hz); 2.75–2.95 (m, 2H); 3.17–3.28 (m, 1H); 3.22 (dd, 1H, *J* = 7.2 and 17.2 Hz); 7.02 (d, 1H, *J* = 4.8 Hz); 7.92 (d, 1H, *J* = 4.8 Hz). ¹³C NMR (100 MHz, CDCl₃, δ/ppm): 18.1 (CH₂); 28.9 (CH₂); 47.0 (CH); 116.7 (C); 123.1 (CH); 138.3 (C); 141.2 (CH); 165.7 (C); 193.4 (CO). GC–MS (*m/z*): 177.0 (M⁺, 37%).

6.1.3.2. 2-(8-oxo-5,6,7,8-tetrahydro-4H-cyclohepta[b]thiophen-7-yl)acetonitrile (21). Compound **21** was synthesized by following general procedure II starting from **19** (1.55 g, 5.96 mmol) in 88% (1.08 g) yield; brown oil. IR (ν/cm⁻¹): 1711 (CO); 2247 (CN). ¹H NMR (400 MHz, CDCl₃, δ/ppm): 1.60–1.80 (m, 2H); 2.08–2.20 (m, 2H); 2.54 (dd, 1H, *J* = 8.0 and 17.2 Hz); 2.77–2.85 (m, 2H); 2.95–3.08 (m, 2H); 6.89 (d, 1H, *J* = 4.8 Hz); 7.49 (d, 1H, *J* = 4.8 Hz). ¹³C NMR (100 MHz, CDCl₃, δ/ppm): 19.3 (CH₂); 24.6 (CH₂); 27.8 (CH₂); 28.6 (CH₂); 45.4 (CH); 118.8 (C); 131.1 (CH); 133.1 (CH); 139.5 (C); 149.8 (C); 192.3 (CO). GC–MS (*m/z*): 205.1 (M⁺, 100%).

6.1.4. General procedure III. Synthesis of acids **22, 23**

A mixture of appropriate nitrile (**20** or **21**, 1 equiv.) and HCl 6 M (23 mL per 2.60 mmol of nitrile) was refluxed at 100 °C for 7 h (TLC). After cooling to room temperature, the dark solution was poured into ice and extracted with CHCl₃. The resulting organic layer was washed with H₂O, dried and evaporated to give a crude residue which was used in the next reaction with no further purification.

6.1.4.1. 2-(6-oxo-5,6-dihydro-4H-cyclopenta[b]thiophen-5-yl)acetic acid (22). Compound **22** was synthesized by following general procedure III starting from **20** (0.46 g, 2.60 mmol) in 70% (0.36 g) yield; orange solid; mp 144 °C. IR (ν/cm⁻¹): 1736; 1650 (CO). ¹H NMR (400 MHz, CDCl₃, δ/ppm): 2.58 (dd, 1H, *J* = 8.8 and 17.2 Hz); 2.65–2.76 (m, 1H); 2.97 (dd, 1H, *J* = 4.0 and 17.2 Hz); 3.28–3.37 (m, 2H); 6.98 (d, 1H, *J* = 4.8 Hz); 7.87 (d, 1H, *J* = 4.8 Hz); 9.51 (bs, 1H). ¹³C NMR (100 MHz, CDCl₃, δ/ppm): 31.1 (CH₂); 35.4 (CH₂); 48.5 (CH); 124.0 (CH); 139.8 (C); 141.3 (CH); 167.2 (C); 177.3 (CO); 197.3 (CO). GC–MS (*m/z*): 196.0 (M⁺, 79%).

6.1.4.2. 2-(8-oxo-5,6,7,8-tetrahydro-4H-cyclohepta[b]thiophen-7-yl)acetic acid (23). Compound **23** was synthesized by following general procedure III starting from **21** (1.10 g, 5.36 mmol) in 88% (1.06 g) yield; black solid; mp 104 °C. IR (ν/cm⁻¹): 1709; 1649 (CO). ¹H NMR (400 MHz, CDCl₃, δ/ppm): 1.52–1.75 (m, 2H); 1.88–2.13 (m, 2H); 2.40 (dd, 1H, *J* = 5.6 and 16.8 Hz); 2.80–3.05 (m, 3H); 3.17–3.28 (m, 1H); 6.86 (d, 1H, *J* = 4.8 Hz); 7.44 (d, 1H, *J* = 4.8 Hz); 10.47 (bs, 1H). ¹³C NMR (100 MHz, CDCl₃, δ/ppm): 24.9 (CH₂); 28.2 (CH₂); 28.6 (CH₂); 35.8 (CH₂); 45.1 (CH); 130.9 (CH); 132.3 (CH); 140.2 (C); 149.5 (C); 178.3 (CO); 194.7 (CO). GC–MS (*m/z*): 224.0 (M⁺, 2%).

6.1.5. General procedure IV. Synthesis of pyridazinones **3, 4**

To a solution of appropriate acid **22** or **23** (1 equiv.) in EtOH (5 mL per 1.00 mmol of acid), hydrazine hydrate (1.3 equiv.) was added and the whole refluxed for 3 h. After cooling to room temperature the solvent was evaporated to give a crude residue which was purified by FC.

6.1.5.1. 2,4,4a,5-tetrahydro-3H-thieno[3',2'-4,5]cyclopenta[1,2-*c*]pyridazin-3-one (3). Compound **3** was synthesized by following general procedure IV starting from **22** (0.36 g, 1.83 mmol) in 66% (0.23 g) yield; brown solid (purification by FC: AcOEt/hexane 9:1); mp 182–185 °C. IR (ν/cm⁻¹): 1660 (CO). ¹H NMR (400 MHz, CDCl₃, δ/ppm): 2.39 (t, 1H, *J* = 16.4 Hz); 2.56 (dd, 1H, *J* = 4.8 and 16.4 Hz); 2.82 (dd, 1H, *J* = 6.8 and 16.4 Hz); 3.25 (dd, 1H, *J* = 7.6 and 16.4 Hz); 3.40–3.50 (m, 1H); 6.90 (d, 1H, *J* = 4.8 Hz); 7.51 (d, 1H, *J* = 4.8 Hz); 8.37 (bs, 1H). ¹³C NMR (100 MHz, CDCl₃, δ/ppm): 32.6 (CH₂); 33.7 (CH₂); 40.7 (CH); 123.2 (CH); 135.0 (CH); 136.2 (C); 156.9 (C); 157.5 (C); 166.8 (CO). GC–MS (*m/z*): 192.1 (M⁺, 100%).

6.1.5.2. 2,4,4a,5,6,7-hexahydro-3H-thieno[3',2'-6,7]cyclohepta[1,2-*c*]pyridazin-3-one (4). Compound **4** was synthesized by following general procedure IV starting from **23** (0.95 g, 4.23 mmol) in 71% (0.66 g) yield; yellow solid (purified by FC: AcOEt/hexane 6:4); mp 155 °C. IR (ν/cm⁻¹): 1681 (CO). ¹H NMR (400 MHz, CDCl₃, δ/ppm): 1.71–1.85 (m, 1H); 1.86–2.00 (m, 3H); 2.39 (dd, 1H, *J* = 12.4 and 17.2 Hz); 2.64 (dd, 1H, *J* = 6.8 and 16.8 Hz); 2.85–2.99 (m, 2H); 3.00–3.10 (m, 1H); 6.83 (d, 1H, *J* = 5.2 Hz); 7.23 (d, 1H, *J* = 5.2 Hz); 8.86 (bs, 1H). ¹³C NMR (100 MHz, CDCl₃, δ/ppm): 24.5 (CH₂); 29.2 (CH₂); 30.1 (CH₂); 33.6 (CH₂); 35.8 (CH); 126.8 (CH); 130.7 (CH); 134.8 (C); 142.3 (C); 152.0 (C); 167.4 (CO). GC–MS (*m/z*): 220.1 (M⁺, 100%).

6.1.6. General procedure V. Synthesis of haloalkyl pyridazinones **5–14**

Method A. To a solution of appropriate pyridazinone **2** or **4** (1 equiv.) in dry DMF (4 mL per 0.92 mmol of pyridazinone), NaH (60% in mineral oil, 3 equiv.) was added at room temperature and the whole stirred for 5 min. The appropriate halogen derivative (3 equiv.) was added, the

resulting mixture stirred at room temperature for 1 h and then poured into cold H₂O. The mixture was extracted with CHCl₃, the organic phase evaporated, to give a crude residue which was purified by FC.

Method B. The appropriate pyridazinone **2** or **3** (1 equiv.), halogen derivative (1.2 equiv.) and tetrabutylammonium hydrogensulfate (0.05 equiv.) were dissolved in CH₂Cl₂ (0.9 mL per 0.76 mmol of pyridazinone) and 28% NaOH (0.9 mL) and H₂O (0.3 mL) were added. The whole was vigorously stirred and heated at 40 °C for 2.5 h. The reaction mixture was then diluted with CH₂Cl₂ (1 mL) and H₂O (0.5 mL) and the phases were separated. The organic phase was dried and evaporated to give a crude residue which was purified by FC (AcOEt/petroleum ether 1:1).

6.1.6.1. 2-(2-bromoethyl)-4,4a,5,6-tetrahydrothieno[3,2-h]cinnolin-3 (2H)-one (5). Compound **5** was synthesized by following general procedure V (method A) starting from **2** (0.10 g, 0.48 mmol) and 1,2-dibromoethane in 93% (0.14 g) yield; yellow solid (FC, AcOEt/petroleum ether 1:1); mp 99–101. °C. IR (ν /cm⁻¹): 1669 (CO). ¹H NMR (400 MHz, CDCl₃, δ/ppm): 1.56–1.70 (m, 1H); 2.12–2.20 (m, 1H); 2.24 (t, 1H, *J* = 15.6 Hz); 2.57–2.90 (m, 4H); 3.50–3.60 (m, 2H); 4.00–4.10 (m, 1H); 4.19–4.29 (m, 1H); 6.80 (d, 1H, *J* = 4.8 Hz); 7.26 (d, 1H, *J* = 5.2 Hz). ¹³C NMR (100 MHz, CDCl₃, δ/ppm): 24.9 (CH₂); 28.9 (CH₂); 30.2 (CH₂); 33.3 (CH); 34.2 (CH₂); 49.0 (CH₂); 127.7 (CH); 128.6 (CH); 131.6 (C); 144.5 (C); 148.7 (C); 165.7 (CO). GC–MS (*m/z*): 313.1 (M⁺).

6.1.6.2. 2-(4-bromobutyl)-4,4a,5,6-tetrahydrothieno[3,2-h]cinnolin-3 (2H)-one (6). Compound **6** was synthesized by following general procedure V (method B) starting from **2** (0.15 g, 0.73 mmol) and 1,4-dibromobutane in 88% (0.22 g) yield; white solid; mp 85 °C. IR (ν /cm⁻¹): 1665 (CO). ¹H NMR (400 MHz, CDCl₃, δ/ppm): 1.55–1.68 (m, 1H); 1.72–1.88 (m, 4H); 2.12–2.21 (m, 1H); 2.21 (t, 1H, *J* = 15.6 Hz); 2.55–2.89 (m, 4H); 3.39 (t, 2H, *J* = 6.4 Hz); 3.65–3.73 (m, 1H); 3.81–3.89 (m, 1H); 6.80 (d, 1H, *J* = 4.8 Hz); 7.25 (d, 1H, *J* = 5.2 Hz). ¹³C NMR (100 MHz, CDCl₃, δ/ppm): 25.0 (CH₂); 26.8 (CH₂); 29.8 (CH₂); 30.2 (CH₂); 33.4 (CH₂); 33.4 (CH); 34.3 (CH₂); 46.9 (CH₂); 127.8 (CH); 128.4 (CH); 131.9 (C); 144.2 (C); 148.1 (C); 165.5 (CO). GC–MS (*m/z*): 340.0 (M⁺, 19%); 342.0 (M⁺ + 2, 19%).

6.1.6.3. 2-(4-bromobutyl)-2,4,4a,5-tetrahydro-3H-thieno[3',2'-4,5]cyclopenta[1,2-c]pyridazin-3-one (7). Compound **7** was synthesized by following general procedure V (method B) starting from **3** (0.10 g, 0.52 mmol) and 1,4-dibromobutane in 82% (0.14 g) yield; white solid; mp 75–83 (dec). IR (ν /cm⁻¹): 1655 (CO). ¹H NMR (400 MHz, CDCl₃, δ/ppm): 1.72–1.90 (m, 4H); 2.35 (t, 1H, *J* = 16.4 Hz); 2.53 (dd, 1H, *J* = 4.0 and 16.0 Hz); 2.80 (dd, 1H, *J* = 6.4 and 16.0 Hz); 3.22 (dd, 1H, *J* = 7.6 and 16.4 Hz); 3.30–3.41 (m, 3H); 3.63–3.71 (m, 1H); 3.84–3.93 (m, 1H); 6.90 (d, 1H, *J* = 5.2 Hz); 7.50 (d, 1H, *J* = 4.8 Hz). ¹³C NMR (100 MHz, CDCl₃, δ/ppm): 26.7 (CH₂); 29.9 (CH₂); 32.5 (CH₂); 33.4 (CH₂); 34.5 (CH₂); 40.8 (CH); 47.2 (CH₂); 123.2 (CH); 134.9 (CH); 136.4 (C); 157.1 (C); 157.5 (C); 164.5 (CO). GC–MS (*m/z*): 246.0 (M⁺ – 81, 93%).

6.1.6.4. 2-(4-bromobutyl)-2,4,4a,5,6,7-hexahydro-3H-thieno[3',2'-6',7]cyclohepta[1,2-c]pyridazin-3-one (8). Compound **8** was synthesized by following general procedure V (method A) starting from **4** (0.40 g, 1.81 mmol) and 1,4-dibromobutane in 20% (0.13 g) yield; yellow oil (FC, AcOEt/hexane 4:6). IR (ν /cm⁻¹): 1668 (CO). ¹H NMR (400 MHz, CDCl₃, δ/ppm): 1.53–1.90 (m, 8H); 2.28 (dd, 1H, *J* = 13.2 and 16.4 Hz); 2.52 (dd, 1H, *J* = 6.4 and 16.4 Hz); 2.82 (t, 2H, *J* = 6.0 Hz); 2.85–2.92 (m, 1H); 3.39 (t, 2H, *J* = 6.0 Hz); 3.70–3.84 (m, 2H); 6.74 (d, 1H, *J* = 5.2 Hz); 7.14 (d, 1H, *J* = 5.2 Hz). ¹³C NMR (100 MHz, CDCl₃, δ/ppm): 24.5 (CH₂); 26.7 (CH₂); 29.5 (CH₂); 29.8 (CH₂); 30.1 (CH₂); 33.3 (CH₂); 34.5 (CH₂); 36.3 (CH); 46.8 (CH₂); 126.9 (CH); 130.7 (CH); 135.0 (C); 142.0 (C); 152.0 (C); 165.3 (CO). GC–MS (*m/z*): 354.0 (M⁺, 39%); 356.0 (M⁺ + 2, 38%).

6.1.6.5. 2-(5-bromopentyl)-4,4a,5,6-tetrahydrothieno[3,2-h]cinnolin-3 (2H)-one (9). Compound **9** was synthesized by following general procedure V (method B) starting from **2** (0.15 g, 0.73 mmol) and 1,5-dibromopentane in 81% (0.21 g) yield; white solid; mp 88 °C. IR (ν /cm⁻¹): 1662 (CO). ¹H NMR (400 MHz, CDCl₃, δ/ppm): 1.37–1.43 (m, 2H); 1.57–1.65 (m, 3H); 1.79–1.86 (m, 2H); 2.12–2.19 (m, 1H); 2.19 (t, 1H, *J* = 16.0 Hz); 2.55–2.92 (m, 4H); 3.33 (t, 2H, *J* = 6.8 Hz); 3.62–3.67 (m, 1H); 3.68–3.75 (m, 1H); 6.80 (d, 1H, *J* = 5.2 Hz); 7.25 (d, 1H, *J* = 5.2 Hz). ¹³C NMR (100 MHz, CDCl₃, δ/ppm): 25.0 (CH₂); 25.1 (CH₂); 27.1 (CH₂); 30.2 (CH₂); 32.3 (CH₂); 33.3 (CH); 33.8 (CH₂); 34.2 (CH₂); 47.5 (CH₂); 127.7 (CH); 128.2 (CH); 131.9 (C); 144.1 (C); 147.9 (C); 165.2 (CO). GC–MS (*m/z*): 354.0 (M⁺, 27%); 356.0 (M⁺ + 2, 28%).

6.1.6.6. 2-(5-bromopentyl)-2,4,4a,5-tetrahydro-3H-thieno[3',2':4,5]cyclopenta[1,2-c]pyridazin-3-one (10). Compound **10** was synthesized by following general procedure V (method B) starting from **3** (0.10 g, 0.52 mmol) and 1,5-dibromopentane in 53% (0.09 g) yield; yellow oil. IR (ν /cm⁻¹): 1660 (CO). ¹H NMR (400 MHz, CDCl₃, δ/ppm): 1.35–1.49 (m, 2H); 1.60–1.71 (m, 2H); 1.80–1.90 (m, 2H); 2.34 (t, 1H, *J* = 16.4 Hz); 2.52 (dd, 1H, *J* = 4.4 and 16.0 Hz); 2.79 (dd, 1H, *J* = 6.8 and 16.0 Hz); 3.22 (dd, 1H, *J* = 7.6 and 16.4 Hz); 3.30–3.40 (m, 3H); 3.60–3.70 (m, 1H); 3.80–3.90 (m, 1H); 6.90 (d, 1H, *J* = 4.8 Hz); 7.50 (d, 1H, *J* = 4.8 Hz). ¹³C NMR (100 MHz, CDCl₃, δ/ppm): 25.2 (CH₂); 27.1 (CH₂); 32.4 (CH₂); 32.5 (CH₂); 33.7 (CH₂); 34.5 (CH₂); 40.8 (CH); 47.8 (CH₂); 123.2 (CH); 134.9 (CH); 136.3 (C); 157.0 (C); 157.5 (C); 164.3 (CO). GC–MS (*m/z*): 340.1 (M⁺, 17%); 342.1 (M⁺ + 2, 17%).

6.1.6.7. 2-(6-bromohexyl)-4,4a,5,6-tetrahydrothieno[3,2-h]cinnolin-3 (2H)-one (11). Compound **11** was synthesized by following general procedure V (method B) starting from **2** (0.15 g, 0.73 mmol) and 1,6-dibromohexane in 86% (0.23 g) yield; yellow solid; mp 83–90 °C (dec.). IR (ν /cm⁻¹): 1666 (CO). ¹H NMR (400 MHz, CDCl₃, δ/ppm): 1.20–1.31 (m, 2H); 1.33–1.42 (m, 2H); 1.55–1.67 (m, 3H); 1.76–1.83 (m, 2H); 2.12–2.25 (m, 2H); 2.55–2.92 (m, 4H); 3.38 (t, 2H, *J* = 6.8 Hz); 3.62–3.71 (m, 1H); 3.75–3.86 (m, 1H); 6.81 (d, 1H, *J* = 4.8 Hz); 7.26 (d, 1H, *J* = 4.8 Hz). ¹³C NMR (100 MHz, CDCl₃, δ/ppm): 24.9 (CH₂); 25.7 (CH₂); 27.8 (CH₂); 27.9 (CH₂); 30.2 (CH₂); 33.3 (CH₂); 33.9 (CH); 34.3 (CH₂); 34.4 (CH₂); 47.8 (CH₂); 127.7 (CH); 128.2 (CH); 131.9 (C); 144.0 (C); 147.9 (C); 165.2 (CO). GC–MS (*m/z*): 369.2 (M⁺, 5%).

6.1.6.8. 2-(6-bromohexyl)-2,4,4a,5-tetrahydro-3H-thieno[3',2':4,5]cyclopenta[1,2-c]pyridazin-3-one (12). Compound **12** was synthesized by following general procedure V (method B) starting from **3** (0.10 g, 0.52 mmol) and 1,6-dibromohexane in 55% (0.10 g) yield; yellow oil. IR (ν /cm⁻¹): 1659 (CO). ¹H NMR (400 MHz, CDCl₃, δ/ppm): 1.26–1.35 (m, 2H); 1.39–1.49 (m, 2H); 1.60–1.69 (m, 2H); 1.71–1.85 (m, 2H); 2.34 (t, 1H, *J* = 16.0 Hz); 2.52 (dd, 1H, *J* = 4.0 and 16.0 Hz); 2.79 (dd, 1H, *J* = 6.8 and 16.0 Hz); 3.21 (dd, 1H, *J* = 7.6 and 16.0 Hz); 3.30–3.40 (m, 3H); 3.60–3.70 (m, 1H); 3.80–3.90 (m, 1H); 6.89 (d, 1H, *J* = 4.8 Hz); 7.50 (d, 1H, *J* = 4.8 Hz). ¹³C NMR (100 MHz, CDCl₃, δ/ppm): 25.8 (CH₂); 27.8 (2 × CH₂); 32.5 (CH₂); 32.7 (CH₂); 33.9 (CH₂); 34.5 (CH₂); 40.8 (CH); 48.1 (CH₂); 123.2 (CH); 134.8 (CH); 136.4 (C); 156.9 (C); 157.4 (C); 164.3 (CO). GC–MS (*m/z*): 354.1 (M⁺, 18%); 356.1 (M⁺ + 2, 19%).

6.1.6.9. 2-(7-bromoheptyl)-4,4a,5,6-tetrahydrothieno[3,2-h]cinnolin-3 (2H)-one (13). Compound **13** was synthesized by following general procedure V (method B) starting from **2** (0.15 g, 0.73 mmol) and 1,7-dibromoheptane in 75% (0.21 g) yield; yellow oil. IR (ν /cm⁻¹): 1660 (CO). ¹H NMR (400 MHz, CDCl₃, δ/ppm): 1.19–1.40 (m, 6H); 1.52–1.65 (m, 3H); 1.70–1.80 (m, 2H); 2.10–2.25 (m, 2H); 2.52–2.89 (m, 4H); 3.29 (t, 2H, *J* = 6.8 Hz); 3.60–3.69 (m, 1H); 3.72–3.81 (m, 1H); 6.78 (d, 1H, *J* = 5.2 Hz); 7.23 (d, 1H, *J* = 5.2 Hz). ¹³C NMR (100 MHz, CDCl₃, δ/ppm): 25.0 (CH₂); 26.4 (CH₂); 27.9 (CH₂); 28.0 (CH₂); 28.4 (CH₂); 30.2 (CH₂); 32.7 (CH₂); 33.3 (CH); 34.0 (CH₂); 34.3 (CH₂); 47.9 (CH₂); 127.7 (CH); 128.2 (CH); 132.0 (C); 144.0 (C); 147.9 (C); 165.3 (CO). GC–MS (*m/z*):

383.1 (M^+ , 6%); 385.1 ($M^+ + 2$, 6%).

6.1.6.10. 2-(7-bromoheptyl)-2,4,4a,5-tetrahydro-3H-thieno[3',2'-4,5]cyclopenta[1,2-c]pyridazin-3-one (14). Compound **14** was synthesized by following general procedure V (method B) starting from **3** (0.10 g, 0.52 mmol) and 1,7-dibromoheptane in 39% (0.07 g) yield; brown oil. IR (ν / cm^{-1}): 1655 (CO). 1H NMR (400 MHz, $CDCl_3$, δ /ppm): 1.20–1.39 (m, 6H); 1.55–1.65 (m, 2H); 1.60–1.72 (m, 2H); 2.33 (t, 1H, $J = 16.0$ Hz); 2.52 (dd, 1H, $J = 4.4$ and 16.4 Hz); 2.78 (dd, 1H, $J = 6.8$ and 16.0); 3.20 (dd, 1H, $J = 8.4$ and 16.4 Hz); 3.29–3.38 (m, 3H); 3.55–3.65 (m, 1H); 3.75–3.87 (m, 1H); 6.88 (d, 1H, $J = 4.8$ Hz); 7.48 (d, 1H, $J = 4.8$ Hz). ^{13}C NMR (100 MHz, $CDCl_3$, δ /ppm): 26.4 (CH_2); 27.9 (CH_2); 28.0 (CH_2); 28.4 (CH_2); 32.5 (CH_2); 32.7 (CH_2); 34.0 (CH_2); 34.5 (CH_2); 40.8 (CH); 48.2 (CH_2); 123.2 (CH); 134.7 (CH); 136.4 (C); 156.9 (C); 157.4 (C); 164.3 (CO). GC–MS (m/z): 368.1 (M^+ , 18%); 370.1 ($M^+ + 2$, 18%).

6.1.7. Synthesis of 2-(4-(bromomethyl)benzyl)-4,4a,5,6-tetrahydrothieno[3,2-h]cinnolin-3(2H)-one (15)

Method C: To a solution of **2** (0.20 g, 0.97 mmol, 1 equiv.) in CH_3CN (12 mL), K_2CO_3 (0.40 g, 2.90 mmol, 3 equiv.), 1,4-bis(bromomethyl)benzene (0.76 g, 2.90 mmol, 3 equiv.) were added and the whole refluxed for 30 h. The reaction mixture was cooled to room temperature, extracted with $CHCl_3$, and the organic phase dried and evaporated, to give a crude residue which was purified by FC (AcOEt/hesane 1:1). 63% (0.24 g) yield; white solid, mp 141 °C. IR (ν / cm^{-1}): 1663 (CO). 1H NMR (400 MHz, $CDCl_3$, δ /ppm): 1.63–1.79 (m, 1H); 2.20–2.37 (m, 2H); 2.62–2.98 (m, 4H); 4.49 (s, 2H); 4.87 (d, 1H, $J = 14.8$ Hz); 5.08 (d, 1H, $J = 14.4$ Hz); 6.88 (d, 1H, $J = 5.2$ Hz); 7.32–7.44 (m, 5H). ^{13}C NMR (100 MHz, $CDCl_3$, δ /ppm): 25.0 (CH_2); 30.3 (CH_2); 33.4 (CH_2); 33.5 (CH); 34.3 (CH_2); 51.7 (CH_2); 127.7 (CH); 128.5 (CH); 128.6 ($2 \times$ CH); 128.7 ($2 \times$ CH); 131.9 (C); 136.8 (C); 137.9 (C); 144.3 (C); 148.2 (C); 165.3 (CO). GC–MS (m/z): 389.0 (M^+).

6.1.8. General procedure VI. Synthesis of compounds 2a-f, 2h-l, 3a-e, 4a.

To a solution of appropriate bromoalkylpyridazinone (1 equiv.) in CH_3CN (3 mL per 0.38 mmol of bromoalkylpyridazinone), the appropriate amine (1.06 equiv.), K_2CO_3 (1.06 equiv.) and KI (2 mg) were added and the whole refluxed for 1 h. The reaction mixture was cooled to room temperature, evaporated and the residue diluted with H_2O . The mixture was extracted with $CHCl_3$, the organic phase dried and evaporated to give a crude residue which was purified by FC ($CHCl_3/CH_3OH$ 9:1).

6.1.9. General procedure VII. Synthesis of fumarate salts.

A solution of the free base (1 equiv.) and fumaric acid (1 equiv.) in CH_3OH (10 mL per 0.13 mmol of free base) was stirred at room temperature for 0.5 h. The solution was evaporated and the crude residue was triturated with ether, filtered and dried to give the fumarate salt of the title compound as amorphous solid.

6.1.9.1. 2-(4-(4-benzylpiperazin-1-yl)butyl)-4,4a,5,6-tetrahydrothieno[3,2-h]cinnolin-3(2H)-one (2a). Compound **2a** was synthesized by following general procedure VI starting from **6** (0.13 g, 0.38 mmol) and *N*-benzylpiperazine in 98% (0.16 g) yield; brown oil. General procedure VII was used to prepare the corresponding fumarate salt. mp (fumarate, white solid) 195–197 °C. IR (ν / cm^{-1}): 1667 (CO). 1H NMR (400 MHz, $CDCl_3$, δ /ppm): 1.40–1.50 (m, 2H); 1.58–1.68 (m, 3H); 2.10–2.25 (m, 2H); 2.30–2.63 (m, 12H); 2.68–2.88 (m, 2H); 3.43 (s, 2H); 3.62–3.70 (m, 1H); 3.78–3.85 (m, 1H); 6.79 (d, 1H, $J = 4.8$ Hz); 7.13–7.25 (m, 6H). ^{13}C NMR (100 MHz, $CDCl_3$, δ /ppm): 23.8 (CH_2); 25.0 (CH_2); 26.1 (CH_2); 30.3 (CH_2); 33.4 (CH); 34.4 (CH_2); 47.8 (CH_2); 52.9 (CH_2); 53.1 ($3 \times$ CH_2); 58.3 (CH_2); 63.0 (CH_2); 127.0 (CH); 127.7 (CH); 128.2 ($3 \times$ CH); 129.2 ($2 \times$ CH); 132.0 (C); 138.1 (C); 144.1 (C); 148.0 (C); 165.4 (CO). HRMS (ESI, m/z): [$M + H$] $^+$ calculated for $C_{25}H_{33}N_4OS$ 437.2375; found 437.2372. Anal. calcd. for $C_{25}H_{32}N_4OS \cdot C_4H_4O_4$: C 63.0, H 6.6, N 10.1;

found: C 63.1, H 6.4, N 10.0.

6.1.9.2. 2-(4-(dimethylamino)butyl)-4,4a,5,6-tetrahydrothieno[3,2-h]cinnolin-3(2H)-one (2b). Compound **2b** was synthesized by following general procedure VI starting from **6** (0.30 g, 0.88 mmol), dimethylamine hydrochloride and K_2CO_3 (2.12 equiv.) in 82% (0.22 g) yield; brown oil. General procedure VII was used to prepare the corresponding fumarate salt. mp (fumarate, white solid) 102–105 °C. IR (ν / cm^{-1}): 1668 (CO). 1H NMR (400 MHz, $CDCl_3$, δ /ppm): 1.50–1.70 (m, 5H); 2.12–2.25 (m, 2H); 2.30 (s, 6H); 2.42–2.50 (m, 2H); 2.55–2.68 (m, 2H); 2.72–2.89 (m, 2H); 3.62–3.72 (m, 1H); 3.80–3.88 (m, 1H); 6.80 (d, 1H, $J = 5.2$ Hz), 7.25 (d, 1H, $J = 5.2$ Hz). ^{13}C NMR (100 MHz, $CDCl_3$, δ /ppm): 23.7 (CH_2); 25.0 (CH_2); 25.8 (CH_2); 30.2 (CH_2); 33.2 (CH); 34.3 (CH_2); 44.8 ($2 \times$ CH_3); 47.4 (CH_2); 58.9 (CH_2); 127.8 (CH); 128.3 (CH); 132.1 (C); 144.3 (C); 148.2 (C); 165.5 (CO). HRMS (ESI, m/z): [$M + H$] $^+$ calculated for $C_{16}H_{24}N_3OS$ 306.1635; found 306.1635. Anal. calcd. for $C_{16}H_{23}N_3OS \cdot C_4H_4O_4$: C 57.0, H 6.5, N 10.0; found: C 56.9, H 6.7, N 10.1.

6.1.9.3. 2-(4-(diethylamino)butyl)-4,4a,5,6-tetrahydrothieno[3,2-h]cinnolin-3(2H)-one (2c). Compound **2c** was synthesized by following general procedure VI starting from **6** (0.20 g, 0.59 mmol), diethylamine in 78% (0.15 g) yield; brown oil. IR (ν / cm^{-1}): 1667 (CO). 1H NMR (400 MHz, $CDCl_3$, δ /ppm): 1.08 (t, 6H, $J = 7.2$ Hz); 1.50–1.70 (m, 5H); 2.13–2.26 (m, 2H); 2.54–2.71 (m, 8H); 2.73–2.89 (m, 2H); 3.63–3.74 (m, 1H); 3.79–3.89 (m, 1H); 6.80 (d, 1H, $J = 5.0$ Hz); 7.25 (d, 1H, $J = 5.0$ Hz). ^{13}C NMR (100 MHz, $CDCl_3$, δ /ppm): 10.6 ($2 \times$ CH_3); 22.7 (CH_2); 25.0 (CH_2); 25.9 (CH_2); 30.2 (CH_2); 33.4 (CH); 34.3 (CH_2); 46.8 ($2 \times$ CH_2); 47.4 (CH_2); 52.1 (CH_2); 127.8 (CH); 128.3 (CH); 131.9 (C); 144.3 (C); 148.3 (C); 165.5 (CO). HRMS (ESI, m/z): [$M + H$] $^+$ calculated for $C_{18}H_{28}N_3OS$ 334.1948; found 334.1949. Anal. calcd. for $C_{18}H_{27}N_3OS$: C 64.8, H 8.2, N 12.6; found: C 65.0, H 8.0, N 12.8.

6.1.9.4. 2-(4-(pyrrolidin-1-yl)butyl)-4,4a,5,6-tetrahydrothieno[3,2-h]cinnolin-3(2H)-one (2d). Compound **2d** was synthesized by following general procedure VI starting from **6** (0.20 g, 0.59 mmol), pyrrolidine in 83% (0.16 g) yield; brown oil. IR (ν / cm^{-1}): 1661 (CO). 1H NMR (400 MHz, $CDCl_3$, δ /ppm): 1.50–1.80 (m, 10H); 2.13–2.23 (m, 2H); 2.45–2.68 (m, 7H); 2.70–2.90 (m, 2H); 3.63–3.72 (m, 1H); 3.79–3.88 (m, 1H); 6.79 (d, 1H, $J = 5.2$ Hz); 7.24 (d, 1H, $J = 5.2$ Hz). ^{13}C NMR (100 MHz, $CDCl_3$, δ /ppm): 23.4 ($2 \times$ CH_2); 25.0 (CH_2); 25.4 (CH_2); 26.1 (CH_2); 30.3 (CH_2); 33.4 (CH); 34.3 (CH_2); 47.6 (CH_2); 54.1 ($2 \times$ CH_2); 56.0 (CH_2); 127.7 (CH); 128.2 (CH); 132.0 (C); 144.1 (C); 148.1 (C); 165.4 (CO). HRMS (ESI, m/z): [$M + H$] $^+$ calculated for $C_{18}H_{26}N_3OS$ 332.1791; found 332.1790. Anal. calcd. for $C_{18}H_{25}N_3OS$: C 65.2, H 7.6, N 12.7; found: C 65.5, H 7.85, N 12.8.

6.1.9.5. 2-(4-(piperidin-1-yl)butyl)-4,4a,5,6-tetrahydrothieno[3,2-h]cinnolin-3(2H)-one (2e). Compound **2e** was synthesized by following general procedure VI starting from **6** (0.20 g, 0.59 mmol) and piperidine in 86% (0.17 g) yield; brown oil. General procedure VII was used to prepare the corresponding fumarate salt. mp (fumarate, white solid) 143 °C. IR (ν / cm^{-1}): 1651 (CO). 1H NMR (400 MHz, $CDCl_3$, δ /ppm): 1.33–1.80 (m, 12H); 2.12–2.25 (m, 2H); 2.30–2.50 (m, 4H); 2.55–2.68 (m, 2H); 2.70–2.89 (m, 3H); 3.63–3.71 (m, 1H); 3.78–3.88 (m, 1H); 6.80 (d, 1H, $J = 5.2$ Hz); 7.25 (d, 1H, $J = 5.2$ Hz). ^{13}C NMR (100 MHz, $CDCl_3$, δ /ppm): 25.2 ($2 \times$ CH_2); 26.1 (CH_2); 30.2 ($2 \times$ CH_2); 33.4 (CH); 34.3 ($2 \times$ CH_2); 47.6 (CH_2); 54.3 ($3 \times$ CH_2); 58.7 (CH_2); 127.7 (CH); 128.2 (CH); 132.0 (C); 144.2 (C); 148.1 (C); 165.4 (CO). HRMS (ESI, m/z): [$M + H$] $^+$ calculated for $C_{19}H_{28}N_3OS$ 346.1948; found 346.1948. Anal. calcd. for $C_{19}H_{27}N_3OS \cdot C_4H_4O_4$: C 59.85, H 6.8, N 9.1; found: C 59.65, H 6.9, N 9.3.

6.1.9.6. 2-(2-(4-benzylpiperazin-1-yl)ethyl)-4,4a,5,6-tetrahydrothieno[3,2-h]cinnolin-3(2H)-one (2f). Compound **2f** was synthesized by following general procedure VI starting from **5** (0.11 g, 0.35 mmol) and *N*-benzylpiperazine in 78% (0.11 g) yield; white solid. General

procedure **VII** was used to prepare the corresponding fumarate salt. mp (fumarate, white solid) 96–102 °C. IR (ν / cm^{-1}): 1653 (CO). ^1H NMR (400 MHz, CDCl_3 , δ /ppm): 1.55–1.65 (m, 1H); 2.10–2.25 (m, 2H); 2.30–2.90 (m, 14H); 3.42 (s, 2H); 3.78–3.87 (m, 1H); 3.88–3.99 (m, 1H); 6.77 (d, 1H, $J = 4.8$); 7.12–7.35 (m, 6H). ^{13}C NMR (100 MHz, CDCl_3 , δ /ppm): 24.0 (CH_2); 30.2 (CH_2); 32.3 (CH); 33.3 (CH_2); 44.4 (CH_2); 52.0 ($4 \times \text{CH}_2$); 54.7 (CH_2); 62.0 (CH_2); 126.0 (CH); 126.7 (CH); 127.1 ($2 \times \text{CH}$); 127.2 (CH); 128.3 ($2 \times \text{CH}$); 131.0 (C); 136.9 (C); 143.1 (C); 147.0 (C); 164.4 (CO). HRMS (ESI, m/z): $[\text{M} + \text{H}]^+$ calculated for $\text{C}_{23}\text{H}_{29}\text{N}_4\text{OS}$ 409.2057; found 409.2059. Anal. calcd. for $\text{C}_{23}\text{H}_{28}\text{N}_4\text{OS} \cdot \text{C}_4\text{H}_4\text{O}_4$: C 61.8, H 6.15 N 10.7; found: C 62.0, H 6.3, N 10.6.

6.1.9.7. 2-(4-((4-benzylpiperazin-1-yl)methyl)benzyl)-4,4a,5,6-tetrahydrothieno[3,2-*h*]cinnolin-3(2H)-one (**2h**). Compound **2h** was synthesized by following general procedure **VI** starting from **15** (0.15 g, 0.38 mmol) and *N*-benzylpiperazine in 73% (0.14 g) yield; white solid. General procedure **VII** was used to prepare the corresponding fumarate salt. mp (fumarate, white solid) 203–205 °C. IR (ν / cm^{-1}): 1659 (CO). ^1H NMR (400 MHz, CDCl_3 , δ /ppm): 1.50–1.64 (m, 1H); 2.06–2.85 (m, 14H); 3.39 (s, 2H); 3.41 (s, 2H); 4.75 (d, 1H, $J = 14.4$ Hz); 4.98 (d, 1H, $J = 14.4$ Hz); 6.75 (d, 1H, $J = 5.2$ Hz); 7.10–7.30 (m, 10H); ^{13}C NMR (100 MHz, CDCl_3 , δ /ppm): 25.0 (CH_2); 30.3 (CH_2); 33.5 (CH); 34.3 (CH_2); 51.8 (CH_2); 53.0 ($4 \times \text{CH}_2$); 62.7 (CH_2); 63.0 (CH_2); 127.0 (CH); 127.7 (CH); 128.2 ($2 \times \text{CH}$); 128.3 ($2 \times \text{CH}$); 128.4 (CH); 129.3 (C); 129.7 (CH); 132.0 (C); 136.4 (C); 137.0 (C); 138.0 (C); 144.1 (C); 148.1 (C); 165.3 (CO). HRMS (ESI, m/z): $[\text{M} + \text{H}]^+$ calculated for $\text{C}_{29}\text{H}_{33}\text{N}_4\text{OS}$ 485.2370; found 485.2372. Anal. calcd. for $\text{C}_{29}\text{H}_{32}\text{N}_4\text{OS} \cdot \text{C}_4\text{H}_4\text{O}_4$: C 66.0, H 6.0, N 9.3; found: C 66.1, H 6.3, N 9.2.

6.1.9.8. 2-(4-(4-benzylpiperazin-1-yl)butyl)-2,4,4a,5-tetrahydro-3H-thieno[3',2'-4,5]cyclopenta[1,2-*c*]pyridazin-3-one (**3a**). Compound **3a** was synthesized by following general procedure **VI** starting from **7** (0.06 g, 0.18 mmol) and *N*-benzylpiperazine in 51% (0.04 g) yield; yellow oil. General procedure **VII** was used to prepare the corresponding fumarate salt. mp (fumarate, white solid) 190–192 °C. IR (ν / cm^{-1}): 1651 (CO). ^1H NMR (400 MHz, CDCl_3 , δ /ppm): 1.42–1.51 (m, 2H); 1.59–1.68 (m, 2H); 2.30–2.55 (m, 11H); 2.78 (dd, 1H, $J = 6.8$ and 16.0 Hz); 3.20 (dd, 1H, $J = 7.6$ and 16.0 Hz); 3.28–3.45 (m, 2H); 3.46 (s, 2H); 3.60–3.70 (m, 1H); 3.81–3.90 (m, 1H); 6.88 (d, 1H, $J = 4.8$ Hz); 7.12–7.26 (m, 5H); 7.48 (d, 1H, $J = 4.8$ Hz). ^{13}C NMR (100 MHz, CDCl_3 , δ /ppm): 22.6 (CH_2); 25.0 (CH_2); 31.4 (CH_2); 33.5 (CH_2); 39.8 (CH); 47.0 (CH_2); 51.7 ($2 \times \text{CH}_2$); 52.0 ($2 \times \text{CH}_2$); 57.2 (CH_2); 61.9 (CH_2); 122.1 (CH); 126.0 (CH); 127.2 ($2 \times \text{CH}$); 128.2 ($2 \times \text{CH}$); 133.7 (CH); 135.4 (C); 136.9 (C); 155.9 (C); 156.4 (C); 163.4 (CO). HRMS (ESI, m/z): $[\text{M} + \text{H}]^+$ calculated for $\text{C}_{24}\text{H}_{31}\text{N}_4\text{OS}$ 423.2213; found 423.2217. Anal. calcd. for $\text{C}_{24}\text{H}_{30}\text{N}_4\text{OS} \cdot \text{C}_4\text{H}_4\text{O}_4$: C 62.4, H 6.4, N 10.4; found: C 62.3, H 6.5, N 10.65.

6.1.9.9. 2-(4-(4-benzylpiperazin-1-yl)butyl)-2,4,4a,5,6,7-hexahydro-3H-thieno[3',2':6,7]cyclohepta[1,2-*c*]pyridazin-3-one (**4a**). Compound **4a** was synthesized by following general procedure **VI** starting from **8** (0.12 g, 0.33 mmol) and *N*-benzylpiperazine in 66% (0.10 g) yield; yellow oil. General procedure **VII** was used to prepare the corresponding fumarate salt. mp (fumarate, white solid) 181 °C. IR (ν / cm^{-1}): 1668 (CO). ^1H NMR (400 MHz, CDCl_3 , δ /ppm): 1.40–1.51 (m, 1H); 1.55–1.70 (m, 2H); 1.73–1.90 (m, 2H); 2.20–2.52 (m, 16H); 2.75–2.90 (m, 2H); 3.44 (s, 2H); 3.65–3.72 (m, 1H); 3.74–3.83 (m, 1H); 6.72 (d, 1H, $J = 5.2$ Hz); 7.12 (d, 1H, $J = 5.2$ Hz); 7.14–7.27 (m, 5H). ^{13}C NMR (100 MHz, CDCl_3 , δ /ppm): 23.7 (CH_2); 24.5 (CH_2); 26.0 (CH_2); 29.4 (CH_2); 30.1 (CH_2); 34.6 (CH_2); 36.2 (CH); 47.7 (CH_2); 52.7 ($2 \times \text{CH}_2$); 53.0 ($2 \times \text{CH}_2$); 58.2 (CH_2); 63.0 (CH_2); 126.8 (CH); 127.1 (CH); 128.2 ($2 \times \text{CH}$); 129.2 ($2 \times \text{CH}$); 130.6 (CH); 135.1 (C); 138.0 (C); 141.8 (C); 151.9 (C); 165.3 (CO). HRMS (ESI, m/z): $[\text{M} + \text{H}]^+$ calculated for $\text{C}_{26}\text{H}_{35}\text{N}_4\text{OS}$ 451.2526; found 451.2528. Anal. calcd. for $\text{C}_{26}\text{H}_{34}\text{N}_4\text{OS} \cdot \text{C}_4\text{H}_4\text{O}_4$: C 63.6 H 6.8, N 9.9; found: C 63.7, H 6.6, N 10.1.

6.1.9.10. 2-(4-(4-((1-(phenylsulfonyl)-1H-indol-4-yl)methyl)piperazin-1-yl)butyl)-4,4a,5,6-tetrahydrothieno[3,2-*h*]cinnolin-3(2H)-one (**2i**). Compound **2i** was synthesized by following general procedure **VI** starting from **6** (0.18 g, 0.53 mmol) and 1-(phenylsulfonyl)-4-(piperazin-1-ylmethyl)-1H-indole in 66% (0.21 g) yield; yellow oil. General procedure **VII** was used to prepare the corresponding fumarate salt. mp (fumarate, white solid) 97–104 °C, dec. IR (ν / cm^{-1}): 1659 (CO); 1373 (SO_2). ^1H NMR (400 MHz, CDCl_3 , δ /ppm): 1.55–1.72 (m, 5H); 2.10–2.30 (m, 2H); 2.50–2.96 (m, 14H); 3.60–3.72 (m, 3H); 3.75–3.83 (m, 1H); 6.76–6.81 (m, 2H); 7.09 (d, 1H, $J = 7.2$ Hz); 7.16–7.21 (m, 1H); 7.23 (d, 1H, $J = 5.2$ Hz); 7.35–7.41 (m, 2H); 7.45–7.49 (m, 1H); 7.50 (d, 1H, $J = 3.6$ Hz); 7.80–7.86 (m, 3H). ^{13}C NMR (100 MHz, CDCl_3 , δ /ppm): 23.4 (CH_2); 24.9 (CH_2); 26.0 (CH_2); 30.2 (CH_2); 33.3 (CH); 34.2 (CH_2); 47.6 (CH_2); 52.6 ($2 \times \text{CH}_2$); 53.0 ($2 \times \text{CH}_2$); 58.0 (CH_2); 60.3 (CH_2); 108.1 (CH); 112.3 (CH); 123.9 (CH); 124.4 (CH); 125.8 (CH); 126.7 (CH); 127.8 (CH); 128.2 (CH); 129.3 ($3 \times \text{CH}$); 130.4 (C); 131.1 (C); 131.8 (C); 133.8 (CH); 134.8 (C); 138.1 (C); 144.2 (C); 148.1 (C); 165.4 (CO). HRMS (ESI, m/z): $[\text{M} + \text{H}]^+$ calculated for $\text{C}_{33}\text{H}_{38}\text{N}_5\text{O}_3\text{S}_2$ 616.2411; found 616.2411. Anal. calcd. for $\text{C}_{33}\text{H}_{37}\text{N}_5\text{O}_3\text{S}_2 \cdot \text{C}_4\text{H}_4\text{O}_4$: C 60.7 H 5.65, N 9.6; found: C 61.0, H 5.8, N 9.7.

6.1.9.11. 2-(5-(4-((1-(phenylsulfonyl)-1H-indol-4-yl)methyl)piperazin-1-yl)pentyl)-4,4a,5,6-tetrahydrothieno[3,2-*h*]cinnolin-3(2H)-one (**2j**). Compound **2j** was synthesized by following general procedure **VI** starting from **9** (0.09 g, 0.25 mmol) and 1-(phenylsulfonyl)-4-(piperazin-1-ylmethyl)-1H-indole in 33% (0.05 g) yield; yellow oil. General procedure **VII** was used to prepare the corresponding fumarate salt. mp (fumarate, white solid) 106–114 °C, dec. IR (ν / cm^{-1}): 1655 (CO); 1372 (SO_2). ^1H NMR (400 MHz, CDCl_3 , δ /ppm): 1.20–1.32 (m, 2H); 1.55–1.72 (m, 5H); 2.10–2.30 (m, 2H); 2.49–2.99 (m, 14H); 3.60–3.70 (m, 3H); 3.75–3.83 (m, 1H); 6.77 (d, 1H, $J = 5.2$ Hz); 6.79 (d, 1H, $J = 3.2$ Hz); 7.08 (d, 1H, $J = 7.2$ Hz); 7.15–7.21 (m, 1H); 7.21 (d, 1H, $J = 5.2$ Hz); 7.34–7.40 (m, 2H); 7.45 (d, 1H, $J = 7.2$ Hz); 7.49 (d, 1H, $J = 3.6$ Hz); 7.79–7.86 (m, 3H). ^{13}C NMR (100 MHz, CDCl_3 , δ /ppm): 24.2 (CH_2); 24.9 (CH_2); 27.7 (CH_2); 30.2 (CH_2); 33.4 (CH); 34.3 (CH_2); 47.7 (CH_2); 51.7 (CH_2); 52.7 (CH_2); 58.0 (CH_2); 60.1 (CH_2); 107.9 (CH); 112.5 (CH); 124.0 (CH); 124.5 (CH); 125.9 (CH); 126.8 ($2 \times \text{CH}$); 127.7 (CH); 128.2 (CH); 129.3 ($2 \times \text{CH}$); 130.4 (C); 130.6 (C); 131.9 (C); 133.8 (CH); 134.9 (C); 138.2 (C); 144.2 (C); 148.1 (C); 165.4 (CO). HRMS (ESI, m/z): $[\text{M} + \text{H}]^+$ calculated for $\text{C}_{34}\text{H}_{40}\text{N}_5\text{O}_3\text{S}_2$ 630.2567; found 630.2569. Anal. calcd. for $\text{C}_{34}\text{H}_{39}\text{N}_5\text{O}_3\text{S}_2 \cdot \text{C}_4\text{H}_4\text{O}_4$: C 61.2, H 5.8, N 9.4; found: C 60.9, H 5.7, N 9.5.

6.1.9.12. 2-(6-(4-((1-(phenylsulfonyl)-1H-indol-4-yl)methyl)piperazin-1-yl)hexyl)-4,4a,5,6-tetrahydrothieno[3,2-*h*]cinnolin-3(2H)-one (**2k**). Compound **2k** was synthesized by following general procedure **VI** starting from **11** (0.10 g, 0.27 mmol) and 1-(phenylsulfonyl)-4-(piperazin-1-ylmethyl)-1H-indole in 20% (0.03 g) yield; yellow oil. General procedure **VII** was used to prepare the corresponding fumarate salt. mp (fumarate, white solid) 117–125 °C, dec. IR (ν / cm^{-1}): 1660 (CO); 1372 (SO_2). ^1H NMR (400 MHz, CDCl_3 , δ /ppm): 1.15–1.33 (m, 5H); 1.40–1.70 (m, 5H); 2.10–2.24 (m, 2H); 2.30–2.90 (m, 13H); 3.55–3.68 (m, 3H); 3.71–3.85 (m, 1H); 6.76 (d, 1H, $J = 5.2$ Hz); 6.80 (d, 1H, $J = 3.6$ Hz); 7.08 (d, 1H, $J = 7.6$ Hz); 7.15–7.20 (m, 1H); 7.21 (d, 1H, $J = 4.8$ Hz); 7.33–7.40 (m, 2H); 7.44 (d, 1H, $J = 7.6$ Hz); 7.48 (d, 1H, $J = 3.6$ Hz); 7.77–7.86 (m, 3H). ^{13}C NMR (100 MHz, CDCl_3 , δ /ppm): 25.0 (CH_2); 26.0 (CH_2); 26.4 (CH_2); 27.0 (CH_2); 27.9 (CH_2); 30.3 (CH_2); 33.4 (CH); 34.4 (CH_2); 47.9 (CH_2); 52.3 (CH_2); 53.0 (CH_2); 58.3 (CH_2); 60.3 (CH_2); 108.0 (CH); 112.5 (CH); 124.0 (CH); 124.4 (CH); 125.9 (CH); 126.8 ($2 \times \text{CH}$); 127.7 (CH); 128.2 (CH); 129.3 ($2 \times \text{CH}$); 130.5 (C); 130.9 (C); 132.0 (C); 133.8 (CH); 134.9 (C); 138.3 (C); 144.1 (C); 147.9 (C); 165.3 (CO). HRMS (ESI, m/z): $[\text{M} + \text{H}]^+$ calculated for $\text{C}_{35}\text{H}_{42}\text{N}_5\text{O}_3\text{S}_2$ 644.2724; found 644.2720. Anal. calcd. for $\text{C}_{35}\text{H}_{41}\text{N}_5\text{O}_3\text{S}_2 \cdot \text{C}_4\text{H}_4\text{O}_4$: C 61.6 H 6.0, N 9.2; found: C 61.8, H 6.1, N 9.4.

6.1.9.13. 2-(7-(4-((1-(phenylsulfonyl)-1H-indol-4-yl)methyl)piperazin-1-yl)heptyl)-4,4a,5,6-tetrahydrothieno[3,2-h]cinnolin-3(2H)-one (**2l**). Compound **2l** was synthesized by following general procedure VI starting from **13** (0.10 g, 0.26 mmol) and 1-(phenylsulfonyl)-4-(piperazin-1-ylmethyl)-1H-indole in 60% (0.10 g) yield; yellow oil. General procedure VII was used to prepare the corresponding fumarate salt. mp (fumarate, white solid) 102–110 °C, dec. IR (ν/cm^{-1}): IR(ν/cm^{-1}): 1655 (CO); 1372 (SO₂). ¹H NMR (400 MHz, CDCl₃, δ/ppm): 1.12–1.32 (m, 8H); 1.42–1.68 (m, 4H); 2.10–2.22 (m, 2H); 2.30–2.88 (m, 13H); 3.55–3.68 (m, 3H); 3.72–3.82 (m, 1H); 6.75 (d, 1H, $J = 5.2$ Hz); 6.80 (d, 1H, $J = 3.6$ Hz); 7.08 (d, 1H, $J = 7.6$ Hz); 7.12–7.19 (m, 1H); 7.21 (d, 1H, $J = 5.2$ Hz); 7.33–7.39 (m, 2H); 7.44 (d, 1H, $J = 7.6$ Hz); 7.49 (d, 1H, $J = 3.6$ Hz); 7.77–7.85 (m, 3H). ¹³C NMR (100 MHz, CDCl₃, δ/ppm): 25.0 (CH₂); 25.7 (CH₂); 26.4 (CH₂); 27.2 (CH₂); 27.9 (CH₂); 28.9 (CH₂); 30.2 (CH₂); 33.4 (CH₂); 34.4 (CH₂); 48.0 (CH₂); 52.0 (CH₂); 52.9 (CH₂); 58.3 (CH₂); 60.2 (CH₂); 108.0 (CH); 112.3 (CH); 124.0 (CH); 124.5 (CH); 124.7 (CH); 126.8 (2 × CH); 127.7 (CH); 128.2 (CH); 129.3 (2 × CH); 130.5 (C); 130.8 (C); 132.0 (C); 133.8 (CH); 134.9 (C); 138.3 (C); 144.1 (C); 147.9 (C); 165.3 (CO). HRMS (ESI, m/z): [M + H]⁺ calculated for C₃₆H₄₄N₅O₃S₂ 658.2880; found 658.2878. Anal. calcd. for C₃₆H₄₃N₅O₃S₂·C₄H₄O₄: C 62.1 H 6.1, N 9.05; found: C 62.0, H 6.4, N 9.3.

6.1.9.14. 2-(4-(4-((1-(phenylsulfonyl)-1H-indol-4-yl)methyl)piperazin-1-yl)butyl)-2,4,4a,5-tetrahydro-3H-thieno[3',2':4,5]cyclopenta[1,2-c]pyridazin-3-one (**3b**). Compound **3b** was synthesized by following general procedure VI starting from **7** (0.04 g, 0.12 mmol) and 1-(phenylsulfonyl)-4-(piperazin-1-ylmethyl)-1H-indole in 87% (0.06 g) yield; yellow oil. General procedure VII was used to prepare the corresponding fumarate salt. mp (fumarate, white solid) 103–111 °C, dec. IR (ν/cm^{-1}): IR(ν/cm^{-1}): 1610 (CO); 1370 (SO₂). ¹H NMR (400 MHz, CDCl₃, δ/ppm): 1.60–1.80 (m, 4H); 2.35 (t, 1H, $J = 16.4$ Hz); 2.51 (dd, 1H, $J = 4.0$ and 16.4 Hz); 2.69–2.75 (m, 10H); 2.79 (dd, 1H, $J = 7.2$ and 16.4 Hz); 3.22 (dd, 1H, $J = 7.6$ and 16.4 Hz); 3.40–3.45 (m, 1H); 3.60–3.75 (m, 3H); 3.80–3.92 (m, 1H); 6.77 (d, 1H, $J = 3.6$ Hz); 6.88 (d, 1H, $J = 4.8$ Hz); 7.09 (d, 1H, $J = 7.2$ Hz); 7.16–7.21 (m, 2H); 7.36–7.42 (m, 2H); 7.45–7.53 (m, 2H); 7.80–7.86 (m, 3H). ¹³C NMR (100 MHz, CDCl₃, δ/ppm): 25.3 (CH₂); 29.7 (CH₂); 32.5 (2 × CH₂); 34.5 (2 × CH₂); 40.9 (CH); 46.8 (CH₂); 52.3 (2 × CH₂); 57.1 (CH₂); 59.7 (CH₂); 107.7 (CH); 112.8 (CH); 123.2 (CH); 124.1 (CH); 124.6 (CH); 126.1 (CH); 126.8 (2 × CH); 129.3 (2 × CH); 130.4 (C); 133.9 (CH); 134.9 (C); 135.0 (CH); 136.2 (C); 138.2 (C); 157.5 (C); 157.8 (C); 164.8 (CO). HRMS (ESI, m/z): [M + H]⁺ calculated for C₃₂H₃₆N₅O₃S₂ 602.2254; found 602.2250. Anal. calcd. for C₃₂H₃₅N₅O₃S₂·C₄H₄O₄: C 60.2 H 5.5, N 9.8; found: C 60.4, H 5.4, N 9.9.

6.1.9.15. 2-(5-(4-((1-(phenylsulfonyl)-1H-indol-4-yl)methyl)piperazin-1-yl)pentyl)-2,4,4a,5-tetrahydro-3H-thieno[3',2':4,5]cyclopenta[1,2-c]pyridazin-3-one (**3c**). Compound **3c** was synthesized by following general procedure VI starting from **10** (0.08 g, 0.23 mmol) and 1-(phenylsulfonyl)-4-(piperazin-1-ylmethyl)-1H-indole in 45% (0.06 g) yield; yellow oil. General procedure VII was used to prepare the corresponding fumarate salt. mp (fumarate, white solid) 107–109 °C. IR (ν/cm^{-1}): IR(ν/cm^{-1}): 1654 (CO); 1372 (SO₂). ¹H NMR (400 MHz, CDCl₃, δ/ppm): 1.15–1.35 (m, 2H); 1.49–1.70 (m, 4H); 2.32 (t, 1H, $J = 16.4$ Hz); 2.40–2.70 (m, 11H); 2.77 (dd, 1H, $J = 6.8$ and 16.0 Hz); 3.20 (dd, 1H, $J = 7.6$ and 16.4 Hz); 3.27–3.42 (m, 1H); 3.55–3.70 (m, 3H); 3.75–3.88 (m, 1H); 6.7 (d, 1H, $J = 4.0$ Hz); 6.87 (d, 1H, $J = 4.8$ Hz); 7.08 (d, 1H, $J = 7.2$ Hz); 7.14–7.19 (m, 1H); 7.34–7.39 (m, 2H); 7.42–7.50 (m, 3H); 7.79–7.83 (m, 3H). ¹³C NMR (100 MHz, CDCl₃, δ/ppm): 24.3 (CH₂); 25.2 (CH₂); 27.7 (CH₂); 32.4 (CH₂); 34.5 (CH₂); 40.8 (CH); 47.9 (CH₂); 51.8 (CH₂); 52.7 (2 × CH₂); 58.0 (CH₂); 60.1 (CH₂); 67.0 (CH₂); 107.9 (CH); 112.5 (CH); 123.2 (CH); 124.0 (CH); 124.5 (CH); 126.0 (CH); 126.8 (2 × CH); 129.3 (2 × CH); 130.5 (C); 130.6 (C); 133.8 (CH); 134.8 (CH); 134.9 (C); 136.4 (C); 138.2 (C); 157.0 (C); 157.5 (C); 164.4 (CO). HRMS (ESI, m/z): [M + H]⁺ calculated for C₃₃H₃₈N₅O₃S₂ 616.2411;

found 616.2411. Anal. calcd. for C₃₃H₃₇N₅O₃S₂·C₄H₄O₄: C 60.7 H 5.65, N 9.6; found: C 60.6, H 5.85, N 9.8.

6.1.9.16. 2-(6-(4-((1-(phenylsulfonyl)-1H-indol-4-yl)methyl)piperazin-1-yl)hexyl)-2,4,4a,5-tetrahydro-3H-thieno[3',2':4,5]cyclopenta[1,2-c]pyridazin-3-one (**3d**). Compound **3d** was synthesized by following general procedure VI starting from **12** (0.07 g, 0.19 mmol) and 1-(phenylsulfonyl)-4-(piperazin-1-ylmethyl)-1H-indole in 62% (0.07 g) yield; yellow oil. General procedure VII was used to prepare the corresponding fumarate salt. mp (fumarate, white solid) 115–119 °C. IR (ν/cm^{-1}): IR(ν/cm^{-1}): 1655 (CO); 1372 (SO₂). ¹H NMR (400 MHz, CDCl₃, δ/ppm): 1.25–1.41 (m, 4H); 1.45–1.68 (m, 4H); 2.30–2.70 (m, 12H); 2.77 (dd, 1H, $J = 6.8$ and 16.0 Hz); 3.19 (dd, 1H, $J = 8.0$ and 16.4 Hz); 3.26–3.36 (m, 1H); 3.55–3.68 (m, 3H); 3.76–3.90 (m, 1H); 6.79 (d, 1H, $J = 3.6$ Hz); 6.87 (d, 1H, $J = 5.2$ Hz); 7.08 (d, 1H, $J = 7.2$ Hz); 7.14–7.19 (m, 1H); 7.33–7.40 (m, 2H); 7.42–7.50 (m, 3H); 7.78–7.85 (m, 3H). ¹³C NMR (100 MHz, CDCl₃, δ/ppm): 25.7 (CH₂); 26.3 (CH₂); 27.0 (CH₂); 27.8 (CH₂); 32.4 (CH₂); 34.5 (CH₂); 40.8 (CH); 48.1 (CH₂); 52.0 (CH₂); 52.8 (CH₂); 58.2 (CH₂); 60.2 (CH₂); 108.0 (CH); 112.5 (CH); 123.2 (CH); 124.0 (CH); 124.5 (CH); 125.9 (CH); 126.8 (2 × CH); 129.3 (2 × CH); 130.5 (C); 130.8 (C); 133.8 (CH); 134.7 (CH); 134.9 (C); 136.4 (C); 138.2 (C); 157.0 (C); 157.4 (C); 164.3 (CO). HRMS (ESI, m/z): [M + H]⁺ calculated for C₃₄H₄₀N₅O₃S₂ 630.2567; found 630.2580. Anal. calcd. for C₃₄H₃₉N₅O₃S₂·C₄H₄O₄: C 61.2, H 5.8, N 9.4; found: C 61.5, H 5.9, N 9.7.

6.1.9.17. 2-(7-(4-((1-(phenylsulfonyl)-1H-indol-4-yl)methyl)piperazin-1-yl)heptyl)-2,4,4a,5-tetrahydro-3H-thieno[3',2':4,5]cyclopenta[1,2-c]pyridazin-3-one (**3e**). Compound **3e** was synthesized by following general procedure VI starting from **14** (0.05 g, 0.14 mmol) and 1-(phenylsulfonyl)-4-(piperazin-1-ylmethyl)-1H-indole in 60% (0.05 g) yield; yellow oil. General procedure VII was used to prepare the corresponding fumarate salt. mp (fumarate, white solid) 120–123 °C. IR (ν/cm^{-1}): IR(ν/cm^{-1}): 1654 (CO); 1371 (SO₂). ¹H NMR (400 MHz, CDCl₃, δ/ppm): 1.12–1.35 (m, 6H); 1.42–1.65 (m, 4H); 2.28–2.70 (m, 12H); 2.77 (dd, 1H, $J = 6.4$ and 16.0 Hz); 3.19 (dd, 1H, $J = 7.6$ and 16.4 Hz); 3.28–3.40 (m, 1H); 3.58–3.62 (m, 3H); 3.80–3.88 (m, 1H); 6.79 (d, 1H, $J = 4.0$ Hz); 6.87 (d, 1H, $J = 4.8$ Hz); 7.08 (d, 1H, $J = 7.2$ Hz); 7.14–7.19 (m, 1H); 7.33–7.40 (m, 2H); 7.42–7.50 (m, 3H); 7.78–7.85 (m, 3H). ¹³C NMR (100 MHz, CDCl₃, δ/ppm): 25.7 (CH₂); 26.4 (CH₂); 27.2 (CH₂); 27.9 (CH₂); 28.9 (CH₂); 32.4 (CH₂); 34.6 (CH₂); 40.8 (CH); 48.2 (CH₂); 52.0 (CH₂); 52.8 (2 × CH₂); 58.2 (CH₂); 60.1 (CH₂); 107.9 (CH); 112.5 (CH); 123.2 (CH); 124.0 (CH); 124.5 (CH); 125.9 (CH); 126.8 (2 × CH); 129.3 (2 × CH); 130.4 (C); 130.8 (C); 133.8 (CH); 134.7 (CH); 134.9 (C); 136.4 (C); 138.2 (C); 156.9 (C); 157.4 (C); 164.3 (CO). HRMS (ESI, m/z): [M + H]⁺ calculated for C₃₅H₄₂N₅O₃S₂ 644.2724; found 644.2721. Anal. calcd. for C₃₅H₄₁N₅O₃S₂·C₄H₄O₄: C 61.6 H 6.0, N 9.2; found: C 61.7, H 6.2, N 9.4.

6.1.10. 2-((4-benzylpiperazin-1-yl)methyl)-4,4a,5,6-tetrahydrothieno[3,2-h]cinnolin-3(2H)-one (**2g**)

To a solution of **2** (0.10 g, 0.48 mmol) in dry ethanol (5 mL), 37% formaldehyde (0.43 mL, 5.76 mmol, 12 equiv.), *N*-benzylpiperazine (0.18 mL, 1.06 mmol, 2.2 equiv) were added and the whole was refluxed under nitrogen atmosphere for 3 h. The reaction mixture was cooled to rt, then the solvent was evaporated under reduced pressure and the residue was taken-up in water and extracted with chloroform. The combined organic phase was dried (Na₂SO₄), filtered and concentrated *in vacuo*, to give a crude residue which was purified by flash chromatography (CH₂Cl₂/CH₃OH 9.5:0.5). 89% (0.17 g) yield; yellow oil. General procedure VII was used to prepare the corresponding fumarate salt. mp (fumarate, white solid) 170–175 °C. IR (ν/cm^{-1}): 1670 (CO). ¹H NMR (400 MHz, CDCl₃, δ/ppm): ¹H NMR (400 MHz, CDCl₃, δ/ppm): 1.67–1.74 (m, 1H); 2.26–2.55 (m, 6H); 2.69–3.00 (m, 7H); 3.38–3.43 (m, 1H); 3.50 (s, 2H); 4.52 (d, 1H, $J = 13.2$ Hz); 5.03 (d, 1H, $J = 13.2$ Hz); 6.87 (d, 1H, $J = 4.8$ Hz); 7.24–7.42 (m, 6H). ¹³C NMR (100 MHz,

CDCl₃, δ/ppm): 24.9 (CH₂); 30.2 (CH₂); 33.4 (CH); 34.3 (CH₂); 50.2 (2 × CH₂); 53.4 (2 × CH₂); 63.1 (CH₂); 68.9 (CH₂); 127.0 (CH); 127.7 (CH); 128.1 (2 × CH); 128.3 (CH); 129.2 (2 × CH); 132.1 (C); 137.8 (C); 144.0 (C); 147.2 (C); 166.8 (CO). HRMS (ESI, *m/z*): [M + H]⁺ calculated for C₂₂H₂₇N₄O₅ 395.1900; found 395.1902. Anal. calcd. for C₂₂H₂₆N₄O₅·C₄H₄O₄: C 61.2, H 5.9, N 11.0; found: C 61.4, H 6.1, N 11.3.

6.2. Biological methods

6.2.1. Cholinesterase inhibition

An already reported methodology was used, reproducing the classical Ellman's spectrophotometric method in a 96-well plate procedure.⁴⁵ All enzymes and reagents were from Sigma-Aldrich Italy. Experiments were performed in 96-well plates (Greiner Bio-One, Kremsmenster, Austria) using a plate reader Infinite M1000 Pro (Tecan, Cernusco sul Naviglio, Italy) and were run in triplicate. Enzyme kinetics were performed by incubating six concentrations of substrate acetylthiocholine (from 0.033 to 0.2 mM) and four concentrations of inhibitor (0–300 nM). The IC₅₀ values and kinetic parameters were obtained by nonlinear regression using Prism software (GraphPad Prism version 5.00 for Windows, GraphPad Software, SanDiego, CA).

6.2.2. Competition binding in human 5-HT_{1A} receptor

Serotonin 5-HT_{1A} receptor competition binding experiments were carried out in a polypropylene 96-well plate and were run in duplicate. In each well was incubated 10 μg of membranes from HEK-5-HT_{1A} #11 cell line prepared in our laboratory (Lot: A005/17-01-2018, protein concentration = 5714 μg/ml), 1 nM [³H]-8-hidroxy-DPAT (162 Ci/mmol, 1 mCi/ml, Perkin Elmer NET929250UC) and compounds studied and standard. Non-specific binding was determined in the presence of 5-HT 10 μM (Sigma H9523). The reaction mixture (V_t: 250 μl/well) was incubated at 37 °C for 120 min, 200 μl was transferred to GF/C 96-well plate (Millipore, Madrid, Spain) pretreated with 0.5% of PEI and treated with binding buffer (50 mM Tris-HCl, 5 mM MgSO₄, pH = 7.4), after was filtered and washed four times with 250 μl wash buffer (50 mM Tris-HCl, pH = 7.4), before measuring in a microplate beta scintillation counter (Microbeta Trilux, PerkinElmer, Madrid, Spain).

6.2.3. Competition binding in human 5-HT₆ receptor

Serotonin 5-HT₆ receptor competition binding experiments were carried out in a polypropylene 96-well plate and were run in duplicate. In each well was incubated 5 μg of membranes from HEK-5-HT₆ cell line prepared in our laboratory (Lot: A001/02-03-2010, protein concentration = 2624 μg/ml), 2 nM [³H]-LSD (82.9 Ci/mmol, 1 mCi/ml, Perkin Elmer NET638250UC) and compounds studied and standard. Non-specific binding was determined in the presence of 5-HT 100 μM (Sigma H9523). The reaction mixture (V_t: 250 μl/well) was incubated at 37 °C for 60 min, 200 μl was transferred to GF/C 96-well plate (Millipore, Madrid, Spain) pretreated with 0.5% of PEI and treated with binding buffer (50 mM Tris-HCl, 10 mM MgCl₂, 0.5 mM EDTA, pH = 7.4), after was filtered and washed four times with 250 μl wash buffer (50 mM Tris-HCl, pH = 7.4), before measuring in a microplate beta scintillation counter (Microbeta Trilux, PerkinElmer, Madrid, Spain).

6.2.4. Competition binding in human 5-HT₇ receptor

Serotonin 5-HT₇ receptor competition binding experiments were carried out in a polypropylene 96-well plate and were run in duplicate. In each well was incubated 2 μg of membranes from HEK-5-HT₇#14 cell line prepared in our laboratory (Lot: A006/21-07-2016, protein concentration = 3316 μg/ml), 2 nM [³H]-SB269970 (34.5 Ci/mmol, 0.25 mCi/ml, Perkin Elmer NET1198U250UC) and compounds studied and standard. Non-specific binding was determined in the presence of clozapine 25 μM (Sigma C6305). The reaction mixture (V_t: 250 μl/well) was incubated at 37 °C for 60 min, 200 μl was transferred to GF/C 96-well plate (Millipore, Madrid, Spain) pretreated with 0.5% of PEI and treated with binding buffer (50 mM Tris-HCl, 4 mM CaCl₂, 1 mM

ascorbic acid, 0.1 mM pargiline, pH = 7.4), after was filtered and washed four times with 250 μl wash buffer (50 mM Tris-HCl, 4 mM CaCl₂, 1 mM ascorbic acid, 0.1 mM pargiline, pH = 7.4) before measuring in a microplate beta scintillation counter (Microbeta Trilux, PerkinElmer, Madrid, Spain).

6.2.5. Functional study in human 5-HT₄ receptor: measurement of Ca⁺² release produced by human serotonin 5-HT₄ receptor activity

Serotonin 5-HT₄ receptor functional experiments were carried out in HeLa-5-HT₄ cell line and were run in duplicate. The day before the assay, 20,000 cells were seeded on a 384 well black plate (Greiner 781091). Using the *FLIPR Calcium 6 Kit* (Molecular Devices R8190), medium was replaced for 25 μl DMEM (Sigma Aldrich D5671) and 25 μl of Calcium 6 dye solution. The cells were incubated for 2 h at 37 °C. After incubation compounds tested and standard were added. Changes in fluorescence owed to intracellular calcium mobilization (λ_{ex} = 480 nm, λ_{em} = 540 nm) were measured using a calcium imaging plate reader system (FDSS7000EX, Hamamatsu®) every second after the establishment of a baseline line. The agonist calcium peak in response to agonist addition occurred from 10 to 20 s following stimulation.

6.3. Molecular modeling

All the studied newly developed compounds as well as the reference ligands (donepezil, tacrine and methiothepin) were manually built within the MOE Builder program and then were parametrized choosing AM1 partial charges as calculation protocol. They were then energy minimized with the Energy Minimize tool included in MOE software, using MMFF94x forcefield.⁵⁴ Root mean square gradient was set equal to 0.0001 (being the root mean square gradient the norm of the gradient times the square root of the number of unfixed atoms allowed to produce a single low-energy conformation for each molecule). All possible enantiomers were taken into account. Since many molecular species exist in solution as an ensemble of tautomers and protonation states, the tool "MOE ligand wash via protonation" command was exploited to create protomers and tautomers using specified pH setting, 7.4 value. In particular, the option dominant was applied, in order to replace the molecule with the dominant protomer/tautomer at the specified pH.

The exploited 4BDS and 7E3H X-ray data, including the hAChE and hBChE in presence of tacrine and donepezil, respectively, were collected from the Protein Data Bank.⁶⁹ The related re-cross docking calculations and the following docking runs, including the newly synthesized compounds, were performed by means of MOE software. Evaluation of the RMSD values between the co-crystallized ligand and the related docking positioning were calculated by Pymol [The PyMOL Molecular Graphics System, Version 1.2r3pre, Schrödinger, LLC]. With regard to the 5-HT₆ protein, a model of the receptor was obtained by means of the AlphaFold protein structure database.^{55,56} In any case, the biological target was energy minimized and refined by means of the MOE QuickPrep tool and protonate3D option, prior to molecular docking calculation.

In the case of docking studies performed on the hAChE and hBChE proteins, the DOCK tool implemented in MOE was exploited, based on the template similarity methodology. The tool works by placing ligands in the active site based on one or more reference structures (templates). It aligns template and input molecules based on triplet matching, which works taking into account the ligand undirected heavy-atoms and projected features. The scoring function incorporates terms for reference/ligand similarity as well as a protein–ligand clash term. In the case of molecular docking studies involving the 5-HT₆ protein model, MOE DOCK tool was applied, referring to the best scored druggable cavity as identified by the MOE Site Finder module, whose details are reported in a previous paper.⁷⁰

In any case, calculation of the enthalpy-based affinity ΔG scoring function allowed to score the generated fifty poses while the Induced Fit method has been exploited to refine the previous poses to the final five docking poses, maintaining the Affinity ΔG as final scoring function for

the definitive pose ranking.

The Affinity ΔG function estimates the enthalpic contribution to the free energy of binding using a linear function:

$$\Delta G = C_{hb} f_{hb} + C_{ion} f_{ion} + C_{hmlig} f_{mli} + C_{hh} f_{hh} + C_{hp} f_{hp} + C_{aa} f_{aa} \quad (1)$$

where the f terms fractionally count atomic contacts of specific types and the C 's are coefficients that weight the term contributions to the affinity estimate.

The individual terms are subscripted with: (i) hb , interactions between hydrogen bond donor–acceptor pairs, (ii) ion , a Coulomb-like term is used to evaluate the interactions between charged groups, (iii) mli : metal ligation (such as those involving Nitrogens/Sulfurs and transition metals), (iv) hh , hydrophobic interactions, for example, between alkane carbons (these interactions are generally favourable); (v) hp , interactions between hydrophobic and polar atoms (these interactions are generally unfavourable), (vi) aa , an interaction between any two atoms. This interaction is weak and generally favourable. Further details are reported in previous papers.^{71,72}

Induced Fit approach allows to maintain flexible protein sidechains within the selected binding site, which are to be included in the refinement stage. The derived docking poses were prioritized by the score values of the lowest energy pose of the compounds docked to the protein structure, as follows: S : the final score (which herein corresponds to affinity ΔG), which is the score of the last stage of refinement, E_{place} : score from the placement stage; E_{score1} and E_{score2} score from rescoring stages 1 and 2; E_{refine} : score from the refinement stage, calculated to be the sum of the van der Waals electrostatics and solvation energies, under the Generalized Born solvation model (GB/VI).

6.4. In silico prediction of ADME properties.

The prediction of all the reported ADME descriptors was performed by means of the Advanced Chemistry Development (ACD) Percepta platform [ACD/Percepta Platform; Advanced Chemistry Development, Inc.: Toronto, ON, Canada, 2015. [(accessed on August 2022)]. Available online: <https://www.acdlabs.com>]. The software prediction are managed based on the implemented training libraries, which refer to different series of derivatives whose pharmacokinetic and safety properties has been experimentally evaluated and reported in the literature.

Declaration of Competing Interest

The authors declare that they have no known competing financial interests or personal relationships that could have appeared to influence the work reported in this paper.

Data availability

The authors do not have permission to share data.

Acknowledgements

Authors thank Prof. Maria Isabel Loza (University of Santiago de C., Spain) for the revision of the manuscript, Dr. Maria Orecchioni, Dr. Massimo Carraro, Mrs. Paola Manconi (University of Sassari) for NMR, GC-MS and HRMS analytical support and Università degli Studi di Sassari: Fondo di Ateneo per la ricerca (FAR 2019 and FAR 2020).

Appendix A. Supplementary material

Supplementary data to this article can be found online at <https://doi.org/10.1016/j.bmc.2023.117256>.

References

- [1] Holmquist M. Alpha beta-hydrolase fold enzymes structures, functions and mechanisms. *Curr Protein Peptide Sci.* 2000;1:209–235. <https://doi.org/10.2174/1389203003381405>.
- [2] Terry Jr AV, Buccafusco JJ. The cholinergic hypothesis of age and Alzheimer's disease-related cognitive deficits: recent challenges and their implications for novel drug development. *J Pharmacol Exp Ther.* 2003;306:821–827. <https://doi.org/10.1124/jpet.102.041616>.
- [3] Ballard CG, Greig NH, Guillozet-Bongaarts AL, Enz A, Darvesh S. Cholinesterases: roles in the brain during health and disease. *Curr Alzheimer Res.* 2005;2:307–318. <https://doi.org/10.2174/1567205054367838>.
- [4] Kořak U, Brus B, Knez D, et al. The magic of crystal structure-based inhibitor optimization: development of a butyrylcholinesterase inhibitor with picomolar affinity and in vivo activity. *J Med Chem.* 2018;61:119–139. <https://doi.org/10.1021/acs.jmedchem.7b01086>.
- [5] De Ferrari G-V, Canales MA, Shin I, Weiner LM, Silman I, Inestrosa NC. A structural motif of acetylcholinesterase that promotes amyloid beta-peptide fibril formation. *Biochemistry.* 2001;40:10447–10457. <https://doi.org/10.1021/bi0101392>.
- [6] García-Ayllón M-S, Small DH, Avila J, Sáez-Valero J. Revisiting the role of acetylcholinesterase in Alzheimer's disease: cross-talk with P-tau and β -amyloid. *Front Mol Neurosci.* 2011;4:1–9. <https://doi.org/10.3389/fnmol.2011.00022>.
- [7] Colovic MB, Krstic DZ, Lazarevic-Pasti TD, Bondznic AM, Vasic VM. Acetylcholinesterase inhibitors: pharmacology and toxicology. *Curr Neuropharm.* 2013;11:315–335. <https://doi.org/10.2174/1570159X11311030006>.
- [8] Sugimoto H, Iimura Y, Yamaniishi Y, Yamatsu K. Synthesis and structure-activity relationships of acetylcholinesterase inhibitors: 1-benzyl-4-[(5,6-dimethoxy-1-oxoindan-2-yl)methyl]piperidine hydrochloride and related compounds. *J Med Chem.* 1995;38:4821–4829. <https://doi.org/10.1021/jm00024a009>.
- [9] Bar-On P, Millard CB, Harel M, et al. Kinetic and structural studies on the interaction of cholinesterases with the anti-Alzheimer drug rivastigmine. *Biochemistry.* 2002;41:3555–3564. <https://doi.org/10.1021/bi020016x>.
- [10] Greenblatt HM, Kryger G, Lewis T, Silman I, Sussman JL. Structure of acetylcholinesterase complexed with (–)-galanthamine at 2.3 Å resolution. *FEBS Lett.* 1999;463:321–326. [https://doi.org/10.1016/S0014-5793\(99\)01637-3](https://doi.org/10.1016/S0014-5793(99)01637-3).
- [11] Yiannopoulou KG, Papageorgiou SG. Current and future treatments in Alzheimer disease: an update. *J. Cen. Nerv. System Dis.* 2020;12:1–12. <https://doi.org/10.1177/1179573520907397>.
- [12] Singh M, Kaur M, Kukreja H, Chugh R, Silakari O, Singh D. Acetylcholinesterase inhibitors as Alzheimer therapy: from nerve toxins to neuroprotection. *Eur J Med Chem.* 2013;70:165–188. <https://doi.org/10.1016/j.ejmech.2013.09.050>.
- [13] De Boer D, Nguyen N, Mao J, Moore J, Sorin EJ. A comprehensive review of cholinesterase modeling and simulation. *Biomolecules.* 2021;11:580. <https://doi.org/10.3390/biom11040580>.
- [14] Huang L-K, Chao S-P, Hu CJ. Clinical trials of new drugs for Alzheimer disease. *J. Biom. Sci.* 2020;27:1–13. <https://doi.org/10.1186/s12929-019-0609-7>.
- [15] Fiorino F, Severino B, Magli E, et al. 5-HT_{1A} receptor: an old target as a new attractive tool in drug discovery from central nervous system to cancer. *J Med Chem.* 2014;57:4407–4426. <https://doi.org/10.1021/jm400533t>.
- [16] Hagen H, Manahan-Vaughan D. The serotonergic 5-HT₄ receptor: a unique modulator of hippocampal synaptic information processing and cognition. *Neurobiol Learn Memory.* 2017;138:145–153. <https://doi.org/10.1016/j.nlm.2016.06.014>.
- [17] Benhamù B, Martín-Fontecha M, Vázquez-Villa H, Pardo L, López-Rodríguez M. Serotonin 5-HT₆ receptor antagonists for the treatment of cognitive deficiency in Alzheimer's disease. *J Med Chem.* 2014;57:7160–7181. <https://doi.org/10.1021/jm5003952>.
- [18] Modica MN, Lacivita E, Intagliata S, et al. Structure–activity relationships and therapeutic potentials of 5-HT₇ receptor ligands: an update. *J Med Chem.* 2018;61:8475–8503. <https://doi.org/10.1021/acs.jmedchem.7b01898>.
- [19] Blattner KM, Canney DJ, Pippin DA, Blass BE. Pharmacology and therapeutic potential of the 5-HT₇ receptor. *ACS Chem Neurosci.* 2019;10:89–119. <https://doi.org/10.1021/acschemneuro.8b00283>.
- [20] Kohen R, Metcalf MA, Khan N, et al. Cloning, characterization, and chromosomal localization of a human 5-HT₆ serotonin receptor. *J Neurochem.* 2002;66:47–56. <https://doi.org/10.1046/j.1471-4159.1996.66010047.x>.
- [21] Riemer C, Borroni E, Levet-Trafit B, et al. Influence of the 5-HT₆ receptor on acetylcholine release in the cortex: pharmacological characterization of 4-(2-bromo-6-pyrrolidin-1-ylpyridine-4-sulfonyl)phenylamine, a potent and selective 5-HT₆ receptor antagonist. *J Med Chem.* 2003;46:1273–1276. <https://doi.org/10.1021/jm021085c>.
- [22] Marcos B, Gil-Bea FJ, Hirst WD, Garcia-Alloza M, Ramirez MJ. Lack of localization of 5-HT₆ receptors on cholinergic neurons: implication of multiple neurotransmitter systems in 5-HT₆ receptor-mediated acetylcholine release. *Eur J Neurosci.* 2006;24:1299–1306. <https://doi.org/10.1111/j.1460-9568.2006.05003.x>.
- [23] Codony X, Vela JM, Ramirez MJ. 5-HT₆ receptor and cognition. *Curr Opin Pharmacol.* 2011;11:94–100. <https://doi.org/10.1016/j.coph.2011.01.004>.
- [24] Marazziti D, Baroni S, Pirone A, et al. Serotonin receptor of type 6 (5-HT₆) in human prefrontal cortex and hippocampus post-mortem: an immunohistochemical and immunofluorescence study. *Neurochem Int.* 2013;62:182–188. <https://doi.org/10.1016/j.neuint.2012.11.013>.
- [25] Helboe L, Egebjerg J, de Jong IEM. Distribution of serotonin receptor 5-HT₆ MRNA in rat neuronal subpopulations: a double in situ hybridization study. *Neuroscience.* 2015;310:442–454.

- [26] Wesolowska A. Potential role of the 5-HT₆ receptor in depression and anxiety: an overview of preclinical data. *Pharmacol Rep.* 2010;62:564–577. [https://doi.org/10.1016/s1734-1140\(10\)70315-7](https://doi.org/10.1016/s1734-1140(10)70315-7).
- [27] Wicke K, Haupt A, Besselov A. Investigational drugs targeting 5-HT₆ receptors for the treatment of Alzheimer's disease. *Expert Opin Invest Drugs.* 2015;24:1515–1528. <https://doi.org/10.1517/13543784.2015.1102884>.
- [28] Wilkinson D, Windfeld K, Colding-Jørgensen E. Safety and efficacy of idalopirdine, a 5-HT₆ receptor antagonist, in patients with moderate Alzheimer's disease (LADDER): a randomised, double-blind, placebo-controlled phase 2 trial. *Lancet Neurol.* 2014;13:1092–1099.
- [29] de Jong IEM, Mørk A. Antagonism of the 5-HT₆ receptor preclinical rationale for the treatment of Alzheimer's disease. *Neuropharmacology.* 2017;125:50–63. <https://doi.org/10.1016/j.neuropharm.2017.07.010>.
- [30] Nirogi RVS, Badange R, Kambhampati R, et al. Design, synthesis and pharmacological evaluation of 4-(piperazin-1-yl-methyl)-N1-arylsulfonyl indole derivatives as 5-HT₆ receptor ligands. *Bioorg Med Chem Lett.* 2012;22:7431–7435. <https://doi.org/10.1016/j.bmcl.2012.10.057>.
- [31] Khoury R, Grysman N, Gold J, Patel K, Grossberg GT. The role of 5-HT₆-receptor antagonists in Alzheimer's disease: an update. *Expert Opin Invest Drugs.* 2018;27:523–533. <https://doi.org/10.1080/13543784.2018.1483334>.
- [32] Atri A, Frölich L, Ballard C, et al. Effect of idalopirdine as adjunct to cholinesterase inhibitors on change in cognition in patients with Alzheimer disease: three randomized clinical trials. *J Am Med Assoc.* 2018;319:130–142. <https://doi.org/10.1001/jama.2017.20373>.
- [33] Albertini C, Salerno A, de Sena Murteira Pinheiro P, Bolognesi ML. From combinations to multitarget-directed ligands: a continuum in Alzheimer's disease polypharmacology. *Med Res Rev.* 2021;41:2606–2633. <https://doi.org/10.1002/med.21699>.
- [34] Więckowska A, Kończakowski M, Bucki A, et al. Novel multi-target-directed ligands for Alzheimer's disease: combining cholinesterase inhibitors and 5-HT₆ receptor antagonists, Design, synthesis and biological evaluation. *Eur J Med Chem.* 2016;124:63–81. <https://doi.org/10.1016/j.ejmech.2016.08.016>.
- [35] Więckowska A, Wichur T, Godyń J, et al. Novel multitarget-directed ligands aiming at symptoms and causes of Alzheimer's disease. *ACS Chem Neurosci.* 2018;9:1195–1214. <https://doi.org/10.1021/acscchemneuro.8b00024>.
- [36] Wichur T, Pasięka A, Godyń J, et al. Discovery of 1-(phenylsulfonyl)-1H-indole-based multifunctional ligands targeting cholinesterases and 5-HT₆ receptor with anti-aggregation properties against amyloid-beta and tau. *Eur J Med Chem.* 2021;225:113783. <https://doi.org/10.1016/j.ejmech.2021.113783>.
- [37] Wichur T, Godyń J, Góral I, et al. Development and crystallography-aided SAR studies of multifunctional BuChE inhibitors and 5-HT₆R antagonists with β -amyloid anti-aggregation properties. *Eur J Med Chem.* 2021;225:113792. <https://doi.org/10.1016/j.ejmech.2021.113792>.
- [38] Więckowski K, Szałaj N, Gryzlo B, et al. Serotonin 5-HT₆ receptor ligands and butyrylcholinesterase inhibitors displaying antioxidant activity-Design, synthesis and biological evaluation of multifunctional agents against Alzheimer's disease. *Int J Mol Sci.* 2022;23:9443. <https://doi.org/10.3390/ijms23169443>.
- [39] Pau A, Catto M, Pinna G, et al. Multitarget-directed tricyclic pyridazinones as G protein-coupled receptor ligands and cholinesterase inhibitors. *ChemMedChem.* 2015;10:1054–1070. <https://doi.org/10.1002/cmdc.201500124>.
- [40] Pinna GA, Curzu MM, Murineddu G, et al. Preparation of thieno[3,2-h]cinnolinones as matrix metalloproteinase inhibitors. *Arch. Pharm. Pharm. Med. Chem.* 2000;333:37–47. [https://doi.org/10.1002/\(sici\)1521-4184\(200002\)333:2/3<37::aid-ardp37>3.0.co;2-v](https://doi.org/10.1002/(sici)1521-4184(200002)333:2/3<37::aid-ardp37>3.0.co;2-v).
- [41] Pau A, Murineddu G, Asproni B, et al. Synthesis and cytotoxicity of novel hexahydrothienocloheptapyridazinone derivatives. *Molecules.* 2009;14:3494–3508. <https://doi.org/10.3390/molecules14093494>.
- [42] Fused thiophene and thiazole derivatives as ROR gamma modulators, K.U. Ravi, H. Subramanya, B. Mallesham, WO 2015/101928 A1.
- [43] Facchetti A, Marks TJ, Takai A, Seger M, Chen Z, Fused thiophene-based conjugated polymers and their use in optoelectronic devices, 2015, US 9,178,160 B1.
- [44] Lazzari P, Zanda M, Sani M. Pharmaceutical compounds, US2014343294 A1.
- [45] Pisani L, Catto M, De Palma A, Farina R, Cellamare S, Altomare CD. Discovery of potent dual binding site acetylcholinesterase inhibitors via homo- and heterodimerization of coumarin-based moieties. *ChemMedChem.* 2017;12:1349–1358. <https://doi.org/10.1002/cmdc.201700282>.
- [46] Rodríguez JJ, Noristani HN, Verkhatsky A. The serotonergic system in ageing and Alzheimer's disease. *Prog Neurobiol.* 2012;99:15–41. <https://doi.org/10.1016/j.pneurobio.2012.06.010>.
- [47] Rebolz H, Friedman E, Castello J. Alterations of expression of the serotonin 5-HT₄ receptor in brain disorders. *Int J Mol Sci.* 2018;19:3581. <https://doi.org/10.3390/ijms19113581>.
- [48] Solas M, Van Dam D, Janssens J, et al. 5-HT(7) receptors in Alzheimer's disease. *Neurochem Int.* 2021;150, 105185. <https://doi.org/10.1016/j.neuint.2021.105185>.
- [49] Verdurand M, Zimmer L. Hippocampal 5-HT(1A) receptor expression changes in prodromal stages of Alzheimer's disease: beneficial or deleterious? *Neuropharmacology.* 2017;123:446–454. <https://doi.org/10.1016/j.neuropharm.2017.06.021>.
- [50] Snięcikowska J, Newman-Tancredi A, Kolaczowski M. From receptor selectivity to functional selectivity: the rise of biased agonism in 5-HT_{1A} receptor drug discovery. *Curr Top Med Chem.* 2019;19:2393–2420. <https://doi.org/10.2174/1568026619666190911122040>.
- [51] <https://www.rcsb.org/structure/7E3H>.
- [52] Nachon F, Carletti E, Ronco C, et al. Crystal structures of human cholinesterases in complex with huprine W and tacrine: elements of specificity for anti-Alzheimer's drugs targeting acetyl- and butyryl-cholinesterase. *Biochem J.* 2013;453:393–399. <https://doi.org/10.1042/BJ20130013>.
- [53] Ramírez D, Caballero J. Is it reliable to take the molecular docking top scoring position as the best solution without considering available structural data? *Molecules.* 2018;23:1038. <https://doi.org/10.3390/molecules23051038>.
- [54] Molecular Operating Environment (MOE); Chemical Computing Group ULC, 1010 Sherbrooke St. West, Suite #910, Montreal, QC, Canada, H3A 2R7, 2021. Available online: <http://www.chemcomp.com/>.
- [55] Jumper J, Evans R, Pritzel A, et al. Highly accurate protein structure prediction with AlphaFold. *Nature.* 2021;596:583–589. <https://doi.org/10.1038/s41586-021-03819-2>.
- [56] Varadi M, Anyango S, Deshpande M, et al. AlphaFold protein structure database: massively expanding the structural coverage of protein-sequence space with high-accuracy models. *Nucleic Acids Res.* 2022;50:D439–D444. <https://doi.org/10.1093/nar/gkab1061>.
- [57] Method of the Year 2021: Protein structure prediction. *Nature Methods* 19 (2022). doi: 10.1038/s41592-021-01380-4.
- [58] Senior AW, Evans R, Jumper J, et al. Improved protein structure prediction using potentials from deep learning. *Nature.* 2020;577:706–710. <https://doi.org/10.1038/s41586-019-1923-7>.
- [59] Franchini S, Manasieva LI, Sorbi C, et al. Synthesis, biological evaluation and molecular modeling of 1-oxa-4-thiaspiro- and 1,4-dithiaspiro[4.5]decane derivatives as potent and selective 5-HT_{1A} receptor agonists. *Eur J Med Chem.* 2017;125:435–452. <https://doi.org/10.1016/j.ejmech.2016.09.05>.
- [60] Prandi A, Franchini S, Manasieva LI, et al. Synthesis, biological evaluation, and docking studies of tetrahydrofuran- cyclopentanone- and cyclopentanol-based ligands acting at adrenergic α -1- and serotonin 5-HT 1A Receptors. *J Med Chem.* 2012;55:23–36. <https://doi.org/10.1021/jm200421e>.
- [61] Franchini S, Prandi A, Baraldi A, et al. 1,3-Dioxolane-based ligands incorporating a lactam or imide moiety: structure-affinity/activity relationship at α 1-adrenoceptor subtypes and at 5-HT_{1A} receptors. *Eur J Med Chem.* 2010;45:3740–3751. <https://doi.org/10.1016/j.ejmech.2010.05.023>.
- [62] Zheng Y, Wu J, Feng X, et al. In silico analysis and experimental validation of ligand extracts from *kadsura longipedunculata* for potential 5-HT_{1A}R agonists. *PLoS One.* 2015;10:e0130055.
- [63] Agnieszka Zagórska A, Kolaczowski M, Bucki A, et al. Structure-activity relationships and molecular studies of novel arylpiperazinylalkyl purine-2,4-diones and purine-2,4,8-triones with antidepressant and anxiolytic-like activity. *Eur J Med Chem.* 2015;97:142–154. <https://doi.org/10.1016/j.ejmech.2015.04.046>.
- [64] Van de Waterbeemd H, Gifford E. ADMET in silico modelling: towards prediction paradise? *Nat Rev Drug Discov.* 2003;2:192–204. <https://doi.org/10.1038/nrd1032>.
- [65] Tonelli M, Espinoza S, Gainetdinov RR, Cichero E. Novel biguanide-based derivatives scouted as TAAR1 agonists: synthesis, biological evaluation, ADME prediction and molecular docking studies. *Eur J Med Chem.* 2017;127:781–792. <https://doi.org/10.1016/j.ejmech.2016.10.058>.
- [66] Sabbadini R, Pesce E, Parodi A, et al. Probing allosteric Hsp70 inhibitors by molecular modelling studies to expedite the development of novel combined F508del CFTR modulators. *Pharmaceuticals.* 2021;14:1296. <https://doi.org/10.3390/ph14121296>.
- [67] Veber DF, Johnson SR, Cheng HY, Smith BR, Ward KW, Kopple KD. Molecular properties that influence the oral bioavailability of drug candidates. *J Med Chem.* 2002;45:2615–2623. <https://doi.org/10.1021/jm020017n>.
- [68] Lipinski CA, Lombardo F, Dominy BW, Feeney PJ. Experimental and computational approaches to estimate solubility and permeability in drug discovery and development settings. *Adv Drug Deliv Rev.* 2001;46:3–26. [https://doi.org/10.1016/S0169-409X\(00\)00129-0](https://doi.org/10.1016/S0169-409X(00)00129-0).
- [69] Berman HM, Battistuz T, Bhat TN, et al. The Protein Data Bank. *Acta Crystallogr D Biol Crystallogr.* 2002;58:899–907. <https://doi.org/10.1107/S0907444902003451>.
- [70] Medjiofack Djeufo FM, Ragazzi E, Urettini M, et al. Magnolol and luteolin inhibition of α -glucosidase activity: kinetics and type of interaction tested by in vitro and in silico studies. *Pharmaceuticals.* 2022;15:205. <https://doi.org/10.3390/ph15020205>.
- [71] Brandas C, Ludovico A, Parodi A, et al. *Biomolecules.* 2021;11:1417. <https://doi.org/10.3390/biom11101417>.
- [72] Francesconi V, Cichero E, Kanov EV, et al. Novel 1-amidino-4-phenylpiperazines as potent agonists at human TAAR1 receptor: rational design, synthesis, biological evaluation and molecular docking studies. *Pharmaceuticals.* 2020;13:391. <https://doi.org/10.3390/ph13110391>.